Integrated Sensing and Communication Signals Toward 5G-A and 6G: A Survey

Zhiqing Wei, *Member, IEEE*, Hanyang Qu, *Member, IEEE*, Yuan Wang, *Member, IEEE*, Xin Yuan, *Member, IEEE*, Huici Wu, *Member, IEEE*, Ying Du, *Member, IEEE*, Kaifeng Han, *Member, IEEE*, Ning Zhang, *Senior Member, IEEE*, and Zhiyong Feng, *Senior Member, IEEE*

***Abstract*—Integrated sensing and communication (ISAC) has the advantages of efficient spectrum utilization and low hardware cost. It is promising to be implemented in the fifth-generation-advanced (5G-A) and sixth-generation (6G) mobile communication systems, having the potential to be applied in intelligent applications requiring both communication and high-accurate sensing capabilities. As the fundamental technology of ISAC, ISAC signal directly impacts the performance of sensing and communication. This article systematically reviews the literature on ISAC signals from the perspective of mobile communication systems, including ISAC signal design, ISAC signal processing, and ISAC signal optimization. We first review the ISAC signal design based on 5G, 5G-A, and 6G mobile communication systems. Then, radar signal processing methods are reviewed for ISAC signals, mainly including the channel information matrix method, spectrum lines estimator method, and super-resolution method. In terms of signal optimization, we summarize peak-to-average power ratio (PAPR) optimization, interference management, and adaptive signal optimization for ISAC signals. This article may provide the guidelines for the research of ISAC signals in 5G-A and 6G mobile communication systems.**

Manuscript received 11 June 2022; revised 16 November 2022; accepted 23 December 2022. Date of publication 9 January 2023; date of current version 23 June 2023. This work was supported in part by the National Key Research and Development Program of China under Grant 2020YFA0711302; in part by the National Natural Science Foundation of China (NSFC) under Grant 62271081, Grant U21B2014, Grant 92267202 and Grant 62271076; in part by the Young Elite Scientists Sponsorship Program by CAST under Grant 2020QNRC001 and Grant 2022QNRC001. *(Corresponding authors: Ying Du; Zhiyong Feng; Huici Wu; Zhiqing Wei.)*

Zhiqing Wei, Hanyang Qu, Yuan Wang, and Zhiyong Feng are with the Key Laboratory of Universal Wireless Communications, Ministry of Education, School of Information and Communication Engineering, Beijing University of Posts and Telecommunications, Beijing 100876, China (e-mail: weizhiqing@bupt.edu.cn; hanyangqu@bupt.edu.cn; wangyuan@bupt.edu.cn; fengzy@bupt.edu.cn).

Xin Yuan is with Data61, CSIRO, Sydney, NSW 2121, Australia (e-mail: xin.yuan@data61.csiro.au).

Huici Wu is with the National Engineering Research Center of Mobile Network Technologies, Beijing University of Posts and Telecommunications, Beijing 100876, China, and also with the Department of Broadband Communiation, Peng Cheng Laboratory, Shenzhen 518066, China (e-mail: dailywu@bupt.edu.cn).

Ying Du is with the Department of Electronic Engineering and Information Science, University of Science and Technology of China, Hefei 230052, China, and also with the Mobile Communications Innovation Center, China Academy of Information and Communications Technology, Beijing 100191, China (e-mail: duying1@caict.ac.cn).

Kaifeng Han is with the Mobile Communications Innovation Center, China Academy of Information and Communications Technology, Beijing 100191, China (e-mail: hankaifeng@caict.ac.cn).

Ning Zhang is with the Department of Electrical and Computer Engineering, University of Windsor, Windsor, ON N9B 3P4, Canada (e-mail: ning.zhang@uwindsor.ca).

Digital Object Identifier 10.1109/JIOT.2023.3235618

***Index Terms*—Fifth-generation-advanced (5G-A), integrated sensing and communication (ISAC), joint sensing and communication, orthogonal frequency-division multiplex (OFDM), orthogonal time frequency space (OTFS), signal design, signal optimization, signal processing, sixth-generation (6G), waveform design.**

I. Introduction

IN THE future fifth-generation-advanced (5G-A) and sixth-generation (6G) mobile communication systems, new intelligent applications and services have emerged, such as machine-type communication (MTC), connected robotics and autonomous driving, and extended reality (XR) [1]. Currently, separated design of sensing and communication cannot achieve high data transmission rate and high-accurate sensing simultaneously and meet the requirements of these new emerging services and applications [2]. Besides, with increasingly scarce spectrum resources, it is difficult to satisfy the spectrum requirements of the new intelligent applications and services.

The integrated sensing and communication (ISAC) system is a unified system providing wireless communication and radar sensing functions. ISAC effectively improves the spectrum utilization and solves the spectrum conflict between radar and communication systems. In addition, ISAC reduces the size and energy consumption of the equipment. Due to the high spectrum efficiency and low hardware cost, academia and industry both pay extensive attention to ISAC technology [3], [4], [5], [6]. As shown in Fig. 1, ISAC technology is expected to be applied in a wide range of intelligent applications that require high data transmission rate and high-accurate sensing capabilities in the era of 5G-A and 6G. With the development and application of millimeter-wave (mmWave) and terahertz (THz) technologies, the frequency bands of communication gradually coincide with these of radar, which promotes the realization of ISAC technology [7].

ISAC technology is developed on the basis of active phased array radar (APAR), since APAR is easily integrated with communication technologies [8]. Mealey [9] proposed that radar pulses can transmit information to space vehicles. In the 1980s, the national aeronautics and space administration (NASA) begin to study the ISAC technology to provide communication and navigation for the space shuttle. A space shuttle program is proposed to support the research of ISAC [10].

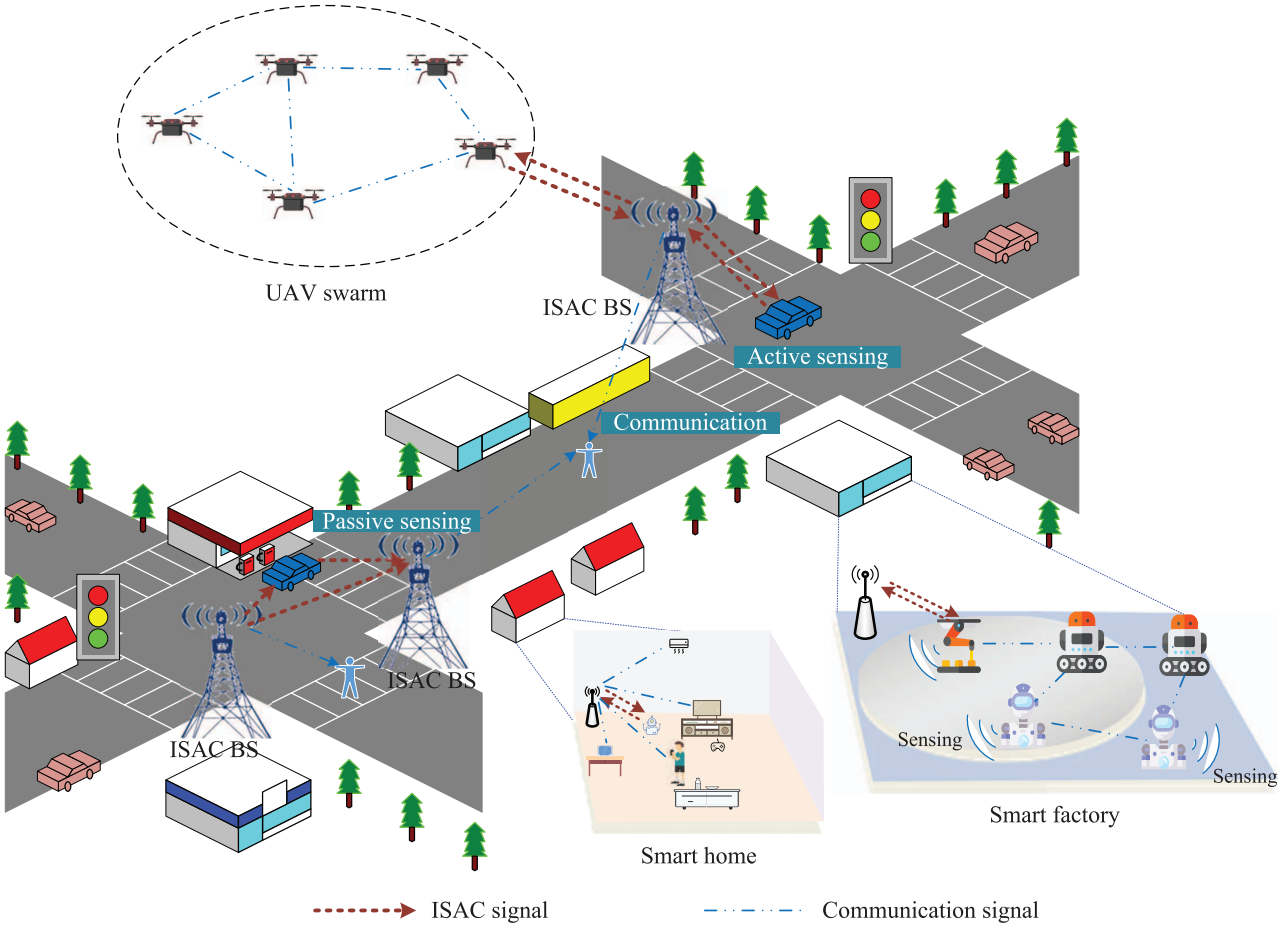

Fig. 1. Application scenarios of ISAC in the future.

Since the 1990s, multiple countries have competed to carry out the research of ISAC technology. The U.S. Office of Naval Research launches the advanced multifunction radio frequency concept program in 1996, trying to integrate radar, electronic warfare, communication, and other functions by using the broadband radio frequency front-end aperture with separated transmitter (TX) and receiver (RX). Germany and Britain have also started the research on ISAC. In 5G-A and 6G, the ISAC-enabled mobile communication systems have attracted much attention [11]. international mobile telecommunication (IMT) 2030 [12] has regarded ISAC as one of the potential technologies of 6G.

ISAC signals, as the basis of ISAC technology, have been studied extensively. Xu et al. [13] applied the direct sequence spread spectrum (DSSS) technique to spread the spectrum of the ISAC system to avoid the jamming between radar and communication. In 2011, Sturm et al. [14] designed an ISAC signal based on orthogonal frequency-division multiplex (OFDM). They demonstrated that OFDM has a high dynamic range of radar imaging [15], which is able to detect multiple targets [16]. In 2013, the shared spectrum access for radar and communications (SSPARCs) project proposed by defense advanced research projects agency (DARPA) promotes the development of ISAC technology [17]. Koslowski et al. [18] designed a filter-bank multicarrier (FBMC)-based ISAC signal and showed that the sensing performance of FBMC is similar to that of OFDM. FBMC-based ISAC signal reduces the overhead of cyclic prefix (CP) and improves the accuracy of velocity estimation. In 2017, the ISAC signal based on orthogonal time frequency space (OTFS) is designed to detect the target with high mobility [19]. Sanson et al. [20] designed generalized frequency-division multiplexing (GFDM)-based ISAC signal, where the signal can reduce out of band (OOB) and use the spectrum without interfering with other users in comparison with OFDM.

Nevertheless, the design of ISAC signal faces great challenges, which are summarized as follows.

1) *ISAC Signal Design:* Communication aims to achieve efficient and reliable data transmission, which requires high spectrum efficiency and the capability of anti-interference and combating channel fading. Radar is to achieve high-resolution target sensing, which requires good autocorrelation, large signal bandwidth, large dynamic range, and large Doppler frequency shift. Thus, the ISAC signal design needs to balance the performance of radar and communication [21], [22].
2) *ISAC Signal Processing:* In order to improve the sensing accuracy with limited computation resources, the design of ISAC signal processing algorithms with high accuracy and low complexity is required.

3) *ISAC Signal Optimization:* It is necessary to design flexible ISAC signal optimization to meet the requirements of sensing and communication in various scenarios.

Facing the above challenges, some existing articles have reviewed the ISAC technology. Hayvaci and Tavli [3] reviewed the ISAC signals from the perspectives of cognitive communication, cognitive radar, and joint cognition of radar and communication systems. Chiriyath et al. [4] defined three levels of ISAC, including coexistence, cooperation, and co-design. In addition, the interference management methods between radar and communication are summarized. Liu et al. [5] comprehensively reviewed the scenarios and key technologies of radar communication coexistence (RCC) and dual function radar communication (DFRC). Zhang et al. [6] summarized radar signal processing algorithms in the ISAC system. They also [23] reviewed the development status and challenges of ISAC in the context of perceptive mobile networks. Wang et al. [24] analyzed the key technologies of ISAC signal in 6G from different application requirements. Tan et al. [25] proposed four typical use cases of ISAC, where the requirements of these use cases are analyzed in detail. The existing ISAC signals are reviewed from the aspect of signal design [26]. The application scenarios and key technologies of ISAC are summarized in [5] and [23]. Recently, Institute of Electrical and Electronics Engineers (IEEE), 3rd Generation Partnership Project (3GPP), IMT-2030, etc., have launched projects on ISAC technology.

The above studies provide a comprehensive overview on the scenarios, requirements, and key technologies of ISAC. However, the ISAC signals from the perspective of 5G-A and 6G mobile communication systems have not been thoroughly reviewed. As 6G takes ISAC as the potential key technology and the ISAC signals are the foundation of ISAC technology, the ISAC signals from the perspective of mobile communication systems of 5G-A and 6G have attracted extensive attention. In this article, we review the ISAC signals, including ISAC signal design, ISAC signal processing, and ISAC signal optimization. The contributions of this article are summarized as follows.

1) *ISAC Signal Design:* This article summarizes ISAC signal design based on the signals in 5G, 5G-A, and 6G mobile communication systems, such as the ISAC signals based on OFDM [8], [27], FBMC [18], [28], GFDM [20], discrete Fourier transform-spread-OFDM (DFT-s-OFDM) [29], and OTFS [30], [31].
2) *ISAC Signal Processing:* The signal processing algorithms for ISAC signal are introduced, including the channel information matrix method, spectrum lines estimator method, and super-resolution method. Then, the detailed signal processing algorithms for the OFDM and OTFS-based ISAC signals are reviewed.
3) *ISAC Signal Optimization:* The ISAC signal optimization methods, including peak-to-average power ratio (PAPR) reduction, interference management, and adaptive signal optimization, are reviewed.

The organization of this article is shown in Fig. 2. In Section II, we review ISAC signal design based on mobile communication systems. In Section III, we review the ISAC signal processing methods. The ISAC signal optimization methods are summarized in Section IV. The future trends are provided in Section V, followed by conclusions in Section VI. The glossary of this article is provided in Table I.

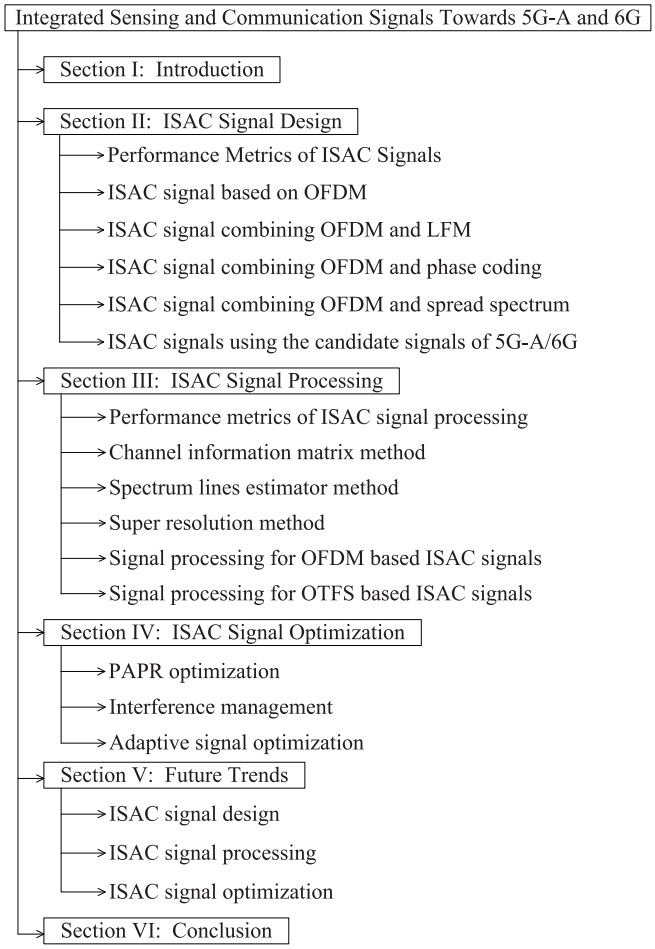

Fig. 2. Organization of this article.

II. ISAC Signal Design

OFDM is the signal of the 4th-generation (4G) and 5G mobile communication systems. The candidate signals of the next-generation mobile communication systems include FBMC, GFDM, DFT-s-OFDM, OTFS, etc. Various ISAC signal design schemes are proposed using the above-mentioned signals. First, we introduce the performance metrics of ISAC signals, followed by the features of OFDM. Then, ISAC signals based on OFDM are introduced. Finally, ISAC signals based on the candidate signals of the next-generation mobile communication system are reviewed.

A. Performance Metrics of ISAC Signals

This section summarizes the performance metrics of ISAC signals, which are used to evaluate the performance of ISAC signals for various application scenarios.

1) *Resolution:* Resolution reveals the ability of ISAC signal to distinguish multiple targets. A small value of resolution of the ISAC signal indicates that the signal has a strong ability to distinguish multiple targets [32].

TABLE I
GLOSSARY

5G-A	Fifth-generation-Advanced	6G	Sixth-generation
APAR	Active Phased Array Radar	AWGN	Additive White Gaussian Noise
BS	Base Station	BER	Bit Error Rate
CP	Cyclic Prefix	CC	Cyclic Cross-correlation
CD-OFDM	Code Division OFDM	CSMA	Carrier Sense Multiple Access
CSMA/CA	Carrier Aware Multiple Access / Collision Avoidance	CSI	Channel State Information
DSSS	Direct Sequence Spread Spectrum	DARPA	Defense Advanced Research Projects Agency
DFRC	Dual-functional Radar-Communication	DoA	Directions of Arrival
DAS	Distributed Antenna System	DIR	Data Information Rate
ESPRIT	Estimating Signal Parameter via Rotational Invariance Techniques	EM	Expectation Maximization
FBMC	Filter-bank Multi-carrier	FM	Frequency Modulation
FRFT	Fractional Fourier Transform	FCW	Forward Collision Warning
GFDM	Generalized Frequency Division Multiplexing	ICI	Inter-carrier Interference
IoV	Internet of Vehicle	ISAC	Integrated Sensing and Communication
ISI	Inter-symbol Interference	KKT	Karush Kuhn Tucher
LRR	Long-Range Radar	MTC	Machine-Type Communication
mmWave	Millimeter-wave	MIMO	Multiple Input Multiple Output
MUSIC	Multiple Signal Classification	MTI	Moving Target Indication
MSK	Minimum-Shift Keying	ML	Maximum Likelihood
MI	Mutual Information	MMSE	Minimum Mean Square Error
MRR	Medium-range Radar	MVDR	Minimum Variance Distortionless Response
MC-DS-CDMA	Multicarrier Direct Sequence CDMA	NASA	National Aeronautics and Space Administration
NC-OFDM	Non-Contiguous-Orthogonal Frequency-Domain Modulation	OFDM	Orthogonal Frequency Division Multiplex
OTFS	Orthogonal Time Frequency Space	OOB	Out of Band
OCDM	Orthogonal Chirp Division Multiplexing	OFDMA	Orthogonal Frequency Division Multiple Access
PAPR	Peak to Average Power Ratio	PSLR	Peak Side Lobe Ratio
PMCW	Phase Modulated Continuous Waveform	PTS	Partial Transmission Sequence
QCQFP	Quadratically Constrained Quadratic Fractional Programming	RCC	Radar-Communication Coexistence
SSPARC	Shared Spectrum Access for Radar and Communications	SIR	Signal to Interference Ratio
SS-OFDM	Spread Spectrum OFDM	SIC	Serial Interference Cancellation
SLM	Selected Mapping	S&C	Schmidl and Cox
SCM	Slow Chirp Modulation	SPR	Subcarrier Power Ratio
SRR	Short-range Radar	SVD	Singular Value Decomposition
TLS-SVD	Total Least Squares-Singular Value Decomposition	THz	Terahertz
V2V	Vehicle-to-Vehicle	XR	Extended Reality

2) *Ambiguity Function:* The ambiguity function is the time–frequency composite autocorrelation function of the complex envelope of ISAC signal. Under the conditions of optimal signal processing, the performance metrics of resolution, ambiguity, accuracy, and clutter suppression of radar sensing are derived via the ambiguity function [33].

3) *Doppler Sensitivity:* Doppler sensitivity is the error of output response of the radar signal processing module and communication demodulation module caused by the Doppler frequency shift. For the signals with high Doppler sensitivity, the sensing output of the radar signal processing module has an intolerable error in the presence of a Doppler frequency shift. Besides, the Doppler

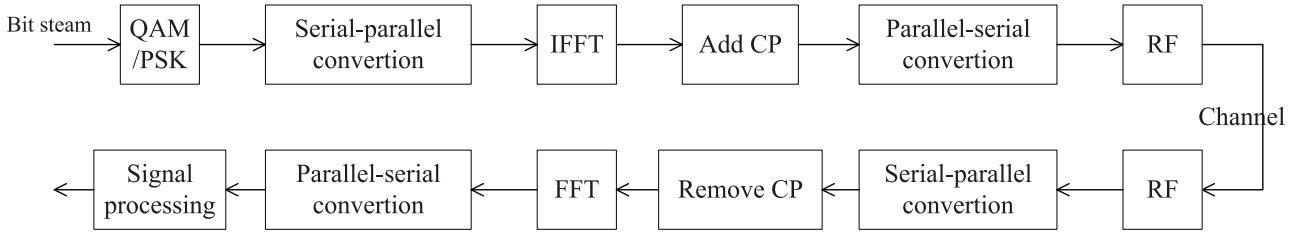

Fig. 3. Signal processing procedure for OFDM signal [8].

frequency shift affects the bit error rate (BER) of the received signals [34], [35].

4) *Doppler Tolerance:* Doppler tolerance is obtained by calculating the cross-correlation between stretched echoes and narrowband approximation signal subtraction in the time domain. Doppler tolerance reveals the maximum velocity detected by the radar, beyond which the velocity estimation will produce intolerable error [36].
5) *PAPR:* PAPR is the ratio of the peak instantaneous power to the average power. A high PAPR will require a high-performance power amplifier, resulting in additional overhead for hardware equipment [37].
6) *Mutual Information (MI):* Communication MI evaluates the channel capacity. Sensing MI is a performance metric that measures the performance of ISAC signals. The sensing MI is defined by the conditional MI of the sensing channel and the echo signal, which is used as the evaluation criterion of sensing performance [21].
7) *Data Information Rate (DIR):* DIR is the information transmission rate, which is used to evaluate the communication efficiency of ISAC signal [38].

B. ISAC Signal Based on OFDM

OFDM is a kind of multicarrier modulation technology, whose signal processing procedure is shown in Fig. 3. The ISAC signal is formulated as [8]

$$s(t) = \sum_{m=0}^{M-1}\sum_{n=0}^{N-1}\left(d(mN+n) \cdot \exp(j2\pi f_n t)\mathrm{rect}\left(\frac{t-mT_{\mathrm{sym}}}{T_{\mathrm{sym}}}\right)\right) \quad (1)$$

where M is the number of symbols, N is the number of subcarriers, T_{sym} is the OFDM symbol duration, f_n is the frequency of the nth subcarrier, $d(mN+n)$ is the modulation symbol, and rect$(\cdot)$ is the rectangular window function.

The subcarriers of OFDM are orthogonal to each other and have the same frequency spacing. The orthogonality reduces inter-carrier interference (ICI) and improves the spectrum efficiency. OFDM facilitates synchronization and equalization, because of the capability of combatting multipath fading. The subcarriers in the ISAC signal using OFDM are orthogonal, and the number and frequency spacing of the subcarriers are flexibly adjusted according to the requirements of various scenarios. As for the sensing capability, a thumbtack-typed ambiguity function is obtained to reduce the delay-Doppler ambiguity for moving target detection and high-resolution imaging [27]. Therefore, OFDM is widely applied in the design of ISAC signals due to its excellent communication and sensing performance.

However, the OFDM signal has high PAPR, distorting the RF front-end [8]. Meanwhile, the mutual interference between the radar echo signal and communication signal, as well as the self-interference between TX and RX, both degrade the performance of radar sensing and communication in the ISAC system, which needs to be solved via signal optimization.

OFDM is usually combined with other modulation methods, such as linear frequency modulation (LFM), phase coding, and spread spectrum to improve the sensing performance of OFDM-based ISAC signals. The OFDM signals combined with these modulation methods have better sensing performance improvement in terms of optimizing ambiguity function, improving anti-interference capability, and reducing PAPR. The ISAC signal combining OFDM and LFM is proposed to improve the resolution of detecting long-distance targets, and the resolution is improved by increasing the time-bandwidth product [39], [40], [41], [42]. ISAC signal combining OFDM and phase coding reduces the PAPR [43], [44], [45], [46]. To enhance the anti-interference capability of ISAC signal in the low SNR regime, ISAC signals combining OFDM and spread spectrum are proposed [47], [48], [49], [50]. The characteristics of OFDM-based ISAC signals are summarized in Table II.

C. ISAC Signal Combining OFDM and LFM

LFM signal is a frequency continuous signal applied in high-accurate radar sensing. In addition, its frequency changes with time. LFM is also called chirp because its frequency changes like a bird call. The echo signal contains delay and Doppler frequency shift. The distance and velocity of the target are estimated through signal processing.

The LFM signal is given by [52]

$$s(t) = \exp\left(j2\pi\left(f_0 t + \frac{1}{2}kt^2\right)\right)\mathrm{rect}\left(\frac{t-T_{\mathrm{LFM}}}{T_{\mathrm{LFM}}}\right) \quad (2)$$

where T_{LFM} is the duration of LFM signal, f_0 is the starting frequency, and k is the chirp rate of LFM.

The instantaneous frequency of the LFM signal increases with time, thereby increasing the time-bandwidth product of the signal and realizing high-resolution and long-distance radar sensing [55]. The ISAC signal combining OFDM and LFM, namely, OFDM-LFM ISAC signal, effectively improves the Doppler sensitivity and reduces the estimation error of velocity [39]. The signal processing procedure for OFDM-LFM

TABLE II
CHARACTERISTICS OF OFDM-BASED ISAC SIGNALS (✓INDICATES THE EXISTENCE OF THE ADVANTAGE)

OFDM based ISAC signal	Design method	Resolution	PAPR reduction	Anti-interference	Secrecy	References
Combination of OFDM and LFM	LFM increases the time-bandwidth product of the signal.	✓				[39]–[42]
Combination of OFDM and phase coding	Phase coding provides a flexible signal design to reduce PAPR.	✓	✓			[43]–[46]
Combination of OFDM and spread spectrum	Spread spectrum improves anti-jamming performance.			✓	✓	[47]–[50]

TABLE III
OFDM-LFM SIGNALS

Category	References	One sentence summary
Carrier modulation	[51], [52]	The subcarrier of OFDM is designed in the form of LFM, and the communication symbol is modulated to the subcarrier.
Non-carrier modulation	[53]	The communication signal is multiplexed at the sideband of an LFM pulse to improve the communication rate.
	[54]	A generalized OFDM-LFM signal is designed to obtain a large time-bandwidth product.

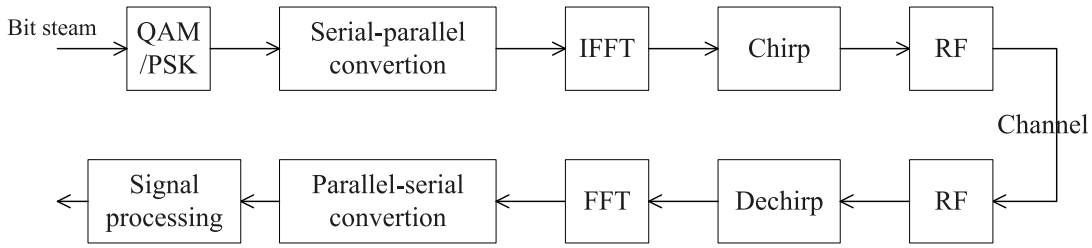

Fig. 4. Signal processing procedure for OFDM-LFM signal [52].

signals is shown in Fig. 4. Compared with the signal processing procedure of OFDM, OFDM-LFM signals have chirp and dechirp processes.

According to the modulation methods, OFDM-LFM signals are classified into two types, namely, carrier modulation and noncarrier modulation, as shown in Table III. The OFDM-LFM signals based on carrier modulation modulate the symbols onto the LFM signals. Noncarrier modulation changes the OFDM-LFM signals, such as changing the sideband or subcarrier arrangement to transmit data [53], [54].

1) Carrier Modulation: Sidney [51] first patented LFM modulation in 1954. Winkler [56] improved LFM modulation in 1962. In the early stage of LFM modulation, binary data 0 and 1 are mapped into positive and negative frequency modulation (FM) frequencies for data transmission. This is approximately regarded as BPSK modulation, where 0 denotes that frequency increases over time, and 1 indicates that frequency decreases with time [52].

The data rate of the above methods is very low. Therefore, high-order modulation schemes are applied to improve the data rate of LFM modulation, such as FSK [42], [57], [58], PSK [39], [40], and QAM [59].

The OFDM-LFM signal based on carrier modulation is expressed as [55]

$$s(t) = \sum_{m=0}^{M-1}\sum_{n=0}^{N-1}\Bigg(d(mN+n)\exp(j2\pi f_n t) \cdot \exp\left(j\pi kt^2\right)\mathrm{rect}\left(\frac{t-mT_{\mathrm{sym}}}{T_{\mathrm{sym}}}\right)\Bigg). \quad (3)$$

Compared with the OFDM signal in (1), there is an additional term $\exp\left(j\pi kt^2\right)$ in the OFDM-LFM signal. To reduce the BER of communication and raise the resolution of distance estimation, a modulation scheme using fractional Fourier transform (FRFT) is proposed in [60]. Small-phase BPSK modulation is applied to improve the concealment of the signal. Compared with traditional BPSK modulation, the phase changes of small phase BPSK are $\pm\varphi$, where $0 < \varphi < \pi/2$ [41].

2) Noncarrier Modulation: Takahashi et al. [53] designed an ISAC signal to improve Doppler tolerance, where the communication signal is multiplexed at the sideband of an LFM pulse. The original LFM pulse is transformed into frequency domain by calculating its FFT, and part of the subcarrier signal in the sideband of the LFM pulse is replaced by complex symbols for communication. Under the above modulation mode, there is no interference between communication and radar. The DIR is proportional to the number of communication subcarriers.

TABLE IV
ISAC SIGNALS COMBINING OFDM AND PHASE CODING

Category	References	One sentence summary
Waveform modulated by phase coding sequence	[43], [44], [27], [61]	Phase coding sequence is modulated to subcarriers to reduce PAPR.
Phase modulated continuous waveform	[45], [62]–[64]	This method combines phase coding sequence and LFM. Phase coding sequence restrains PAPR and LFM provides good velocity estimation performance.

TABLE V
PERFORMANCE COMPARISON OF PHASE CODING SEQUENCES

Phase code	Computational complexity of encoding	Sidelobe level of the autocorrelation function	Envelope of signal
Biphase code	Low	High	Low
Code coding	Medium	Medium	Low
Amplitude and phase modulation	High	Close to zero	Medium
Complementary code	High	Zero between symbols	Low

The large time-bandwidth product of the OFDM-LFM signal improves the sensing resolution. To obtain the signal with a large time-bandwidth product and a suitable signal envelope, Dash et al. [54] proposed a generalized OFDM-LFM signal design, which combines LFM and OFDM signals to achieve a high resolution of distance and velocity estimation. They interleaved zeros in the input sequence to generate a new sequence. Then, other sequences are generated by shifting the new sequence. Therefore, the above sequences are orthogonal. Assuming that the input sequence is $x_p[n]$, as shown in (4), with N discrete spectral components, the input sequence is interleaved by $K-1$ zeros between the two components to form. A new data sequence $x_1[n]$ is obtained with the above method. Then, $x_1[n]$, as shown in (5), is cyclically shifted to generate $x_2[n]\ldots x_K[n]$, as shown in (6). The new K input sequences are calculated by NK points IDFT to get the signals in the time domain which occupy NK subcarriers. However, only the N subcarriers are used to transmit data. Since the input sequence is obtained by cyclic shift, the subcarriers used by data sequences, $x_2[n]\ldots x_K[n]$, are shifted with frequency spacing of Δf. The insertion of zero sequences reduces the peak power of the signal, reducing PAPR. Two adjacent signals are distinguished according to the shift of the used subcarriers. However, the NK subcarriers only carry N modulation symbols.

$$x_p[n] = \{x[0], x[1], x[2], \ldots, x[N-1]\} \tag{4}$$

$$x_1[n] = \{x[0], 0_1, 0_2, \ldots, 0_K, x[1], 0_1, 0_2, \ldots, 0_K, \ldots, x[N-1], 0_1, 0_2, \ldots, 0_K\} \tag{5}$$

$$x_K[n] = \{0_1, 0_2, \ldots, 0_K, x[0], 0_1, 0_2, \ldots, 0_K, x[1], \ldots, 0_1, 0_2, \ldots, 0_K, x[N-1]\}. \tag{6}$$

D. ISAC Signal Combining OFDM and Phase Coding

OFDM signal based on phase coding optimizes the peak sidelobe ratio (PSLR), improving signal envelope performance of the ambiguity function [43]. The specific phase sequence is modulated to the subcarriers of OFDM after constellation mapping. Existing schemes are divided into two cases, namely, direct phase coding sequence modulation and phase modulated continuous waveform (PMCW). The combination of phase coding and LFM, as shown in Table IV, realizes a high time-bandwidth product and reduces PAPR.

1) Direct Phase Coding Sequence Modulation: A phase coding sequence with high autocorrelation reduces the sidelobe level of ambiguity function. The selection of phase coding sequence affects the performance of radar sensing. Commonly used phase coding sequences include biphase code, polyphase code, amplitude and phase modulation code (i.e., Huffman code), and complimentary code. The comparison of these phase coding sequences is shown in Table V.

The OFDM signal combined with phase coding is

$$s(t) = \sum_{n=0}^{N-1}\sum_{m=0}^{M-1} a_{nm}\exp(j2\pi f_n t)\mathrm{rect}\left(\frac{t-mt_b}{t_b}\right) \tag{7}$$

where t_b is the duration of the phase code, and a_{nm} is the phase-coded communication symbol [43]. The signal processing procedure for phase-coded OFDM signal is shown in Fig. 5. Compared with OFDM, the bit stream is modulated with a phase coding sequence prior to QAM/PSK. A dephasing coding module is added at the communication RX.

ISAC signals based on phase coding have been studied extensively [27], [43], [44], [61], [69]. Hu et al. [27] applied random sequences to design ISAC signals that meet the requirements of radar and communication. The deserialized digital sequence is modulated in the corresponding subcarriers, and the information required for radar and communication is extracted at the RX, respectively.

A phase-coded OFDM signal design for a single scattering point target is proposed in [43]. The OFDM signal comprises N subcarriers, and the bit stream is mapped onto an M-bits sequence. They also proposed a radar signal processing algorithm that achieves distance and velocity estimation with high resolution and high DIR [69].

Traditional pseudo-random sequences, such as maximum length linear shift register sequences (m-sequence) and Gold

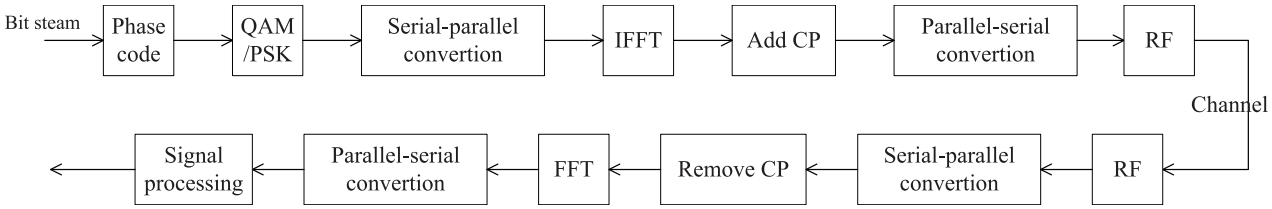

Fig. 5. Signal processing procedure for phase-coded OFDM signal [43].

TABLE VI
ISAC SIGNAL COMBINING OFDM AND SPREAD SPECTRUM

Categories of spread spectrum sequences	References	One sentence summary
Gold sequence	[48], [49], [65], [66]	Gold sequence is the best coding sequence to reduce the peak of cross-ambiguity function.
Minimum-shift keying (MSK) sequence	[67], [68]	ISAC signal based on MSK sequence has a strong correlation.
Multi-carrier direct sequence	[50]	ISAC signal based on multi-carrier direct sequence obtains ideal ambiguity function and low PAPR.

sequences, have good autocorrelation. However, their cross-correlation is not ideal. Moreover, the length of the nth-order m-sequences and Gold sequences is $2^n - 1$. They have a limited number of sequence types and cannot be selected randomly. Therefore, a large number of literature have paid attention to chaotic sequences, which are pseudorandom and only related to the initial state and free parameters. Zhao et al. [44] designed a phase-coded OFDM signal using chaotic sequences, which has a large time-bandwidth product. They proposed a method to extract phase code sequences from chaotic sequences with a good correlation. Then, they proposed the method of subcarrier weighting to reduce the PAPR of the signal. Besides, the signal design has high flexibility to support different application scenarios [44]. Recently, Qi et al. [61] proposed the ISAC signal combining OFDM and phase coding with complete complementary codes, which achieves a high DIR and accurate target detection.

2) Phase Modulated Continuous Waveform: PMCW provides high-resolution sensing. The ambiguity function of PMCW is sharp pushpin type, so that the distance-Doppler coupling is reduced [62], [63]. Moreover, PMCW is easily implemented.

Dokhanchi et al. proposed an automotive ISAC system based on a multicarrier-PMCW (MC-PMCW). MC-PMCW reduces the modulation complexity of the PMCW signal. Due to the PMCW, the proposed signal improves the anti-noise and anti-interference performance of OFDM signal [45].

In the scenario of MTC, the multiplexing strategy is applied to the ISAC system to improve the identifiability of parameters. Dokhanchi et al. embedded communication symbols into PMCW to reduce distance-Doppler ambiguity. At the TX, the sampled sensing and communication sequences are modulated with differential phase shift keying (DPSK) in the frequency domain and transformed to time domain through IFFT [70], [71].

ISAC signal based on LFM or phase coding alone cannot satisfy the extremely high requirements of sensing and communication. Hence, combining phase coding and LFM has attracted widespread attention [46]. Related designs appear in the ISAC-enabled automotive radars. In [46], a group delay filter is applied to process radar echo signals with inconsistent phase coding. The signal-to-interference ratio (SIR) is efficiently enhanced. The RX uses stretching processing to reduce the sampling requirements of the received signal. This method allows the RX to preserve phase coding through dechirp processing because of the transmitted phase-encoded LFM signal.

E. ISAC Signal Combining OFDM and Spread Spectrum

Spread spectrum technology has the advantages of high confidentiality, low power spectral density, and anti-interference capability. The combination of OFDM and spread spectrum, namely, spread spectrum-OFDM (SS-OFDM), reduces the PAPR of OFDM signal. Among the spread spectrum technologies, DSSS is widely applied in the design of ISAC signals. In addition, the selection of spread spectrum sequences directly impacts the performance of ISAC signals, as shown in Table VI.

The implementation process of SS-OFDM is provided as follows. The communication data are first modulated at the TX and then spread with a spread spectrum sequence. Then, the CP is added after IFFT. At the RX, with the processes of FFT, demodulation, and despreading, the original communication data is recovered [47], [72]. The SS-OFDM signal is given by [66]

$$s(t) = \sum_{m=0}^{M-1}\sum_{n=0}^{N-1}\sum_{p=0}^{P-1}\left(d(mN+n)a_m(p)\exp(j2\pi f_n t) \cdot \mathrm{rect}\left(\frac{t - pt_c - mT_{sym}}{T_{sym}}\right)\right) \tag{8}$$

where P is the length of the spread spectrum sequence. $a_m(p)$ is the pth spread spectrum code on the mth OFDM symbol, with the value of ± 1. t_c is the duration of a spread spectrum code. The signal processing procedure for SS-OFDM signals is shown in Fig. 6. Compared with OFDM, the modulation

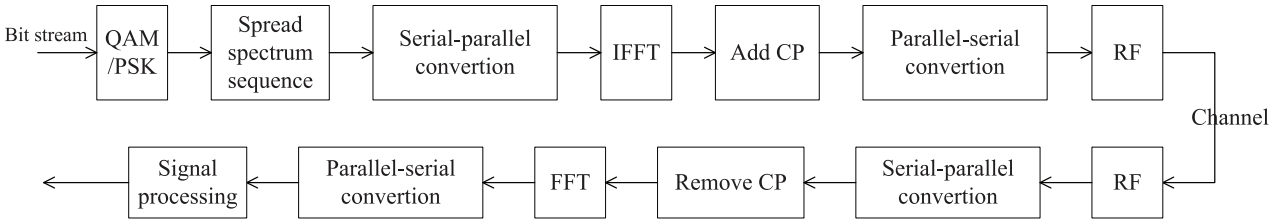

Fig. 6. Signal processing procedure for SS-OFDM signal [66].

symbols are multiplied by the spread spectrum sequence. A despread spectrum module is added at the communication RX.

The follow-up studies have shown that the spread factor affects the sidelobes of the ranging ambiguity function. The Gold sequence is a commonly used spread spectrum sequence, which efficiently reduces the peak of the cross-ambiguity function [65], [66]. The OFDM signal combining spread spectrum and LFM is proposed to improve the resolution of the ISAC signal. The signal design ensures the orthogonality of the signal at the RX and has a large time-bandwidth product [49].

In addition to the Gold sequence, ISAC signals using minimum-shift keying (MSK) and DSSS are designed in [67] and [68]. The MSK signal has the advantage of strong correlation [68]. Besides, the optimization method of MSK at the TX and the method to increase the PSLR at the RX are proposed, which effectively suppress the sidelobe level with sacrificing DIR.

The ISAC signal using multicarrier direct sequence is proposed to obtain an ideal ambiguity function and low PAPR [50]. The subset of M subcarriers uses scrambling codes and orthogonal variable spread factor codes to reduce the correlation between subcarriers. Communication and radar functions are isolated due to the application of scrambling codes, reducing interference between radar and communication.

F. ISAC Signals Using the Candidate Signals of 5G-A/6G

FBMC, GFDM, DFT-s-OFDM, and OTFS are proposed to solve the problems of Doppler sensitivity, high CP overhead, and high PAPR of OFDM [29]. Another candidate signal for the future mobile communication system, namely, universal filtered multicarrier (UFMC), has a higher OOB than OFDM, GFDM, and FBMC, which is rarely used to design ISAC signals. In this section, we introduce the ISAC signals using the candidate signals of 5G-A/6G.

1) FBMC: Different from the complex input data of OFDM, the data stream of FBMC applies real data. FBMC applies prototype filters to ensure orthogonality between subcarriers, thereby avoiding the overhead of CP [28]. The expression of the FBMC signal is

$$s(t)=\sum_{n=0}^{N-1}\sum_{m=0}^{M-1}\Bigg(d(mN+n)g_n(t)\cdot\exp(j2\pi f_n t)\mathrm{rect}\left(\frac{t-mT_{\mathrm{sym}}}{T_{\mathrm{sym}}}\right)\Bigg) \quad (9)$$

where $g_n(t)$ is the prototype filter of each subcarrier. Compared with (1), there is a term $g_n(t)$ for each subcarrier, which is the prototype filter.

In terms of communication, FBMC has no CP and achieves higher spectrum efficiency than OFDM. In terms of radar sensing, FBMC has a pushpin ambiguity function. Due to the characteristics of large bandwidth, FBMC attains the distance resolution equivalent to OFDM. In addition, FBMC does not have the sidelobes brought by CP, and its Doppler bandwidth is larger than OFDM, thereby improving the estimation performance of distance and velocity [18]. The orthogonality between subcarriers is destroyed by the filters. Therefore, the QAM symbol carried by the FBMC signal is not easy to be demodulated. Moreover, the bandwidth of the filter is narrow and there is a long tail in the time domain, which is also one of the disadvantages of FBMC signals.

2) GFDM: GFDM divides subcarriers into multiple groups and adds a filter to each group. The filter of GFDM is wider in the frequency domain than that of FBMC, so that the tail of the filter in the time domain is shorter. The GFDM signal is

$$s(t)=\sum_{n=0}^{N-1}\sum_{m=0}^{M-1}\Bigg(d(mN+n)g_{k,\mathrm{GFDM}}(t)\cdot\exp(j2\pi f_n t)\mathrm{rect}\left(\frac{t-mT_{\mathrm{sym}}}{T_{\mathrm{sym}}}\right)\Bigg) \quad (10)$$

where $g_{k,\mathrm{GFDM}}(t)$ is the filter used for the kth group of subcarriers, which has wide bandwidth to support multiple subcarriers [73]. Compared with (1), there is a term $g_{k,\mathrm{GFDM}}(t)$, which is the filter for kth group of subcarriers. The filter of GFDM is simpler to implement compared with that of FBMC. The modulation method of the GFDM signal is to modulate block-like time–frequency resources. Compared with other signals, it has a more flexible frame structure. However, the complex receiving algorithm is required to eliminate inter-symbol interference (ISI) and ICI. The filters preserve the circular property of the signals in both time and frequency domains [73]. Therefore, the severe mutual interference is avoided and the OOB is reduced. The performance of communication and sensing using OFDM and GFDM signals is analyzed in [20], where GFDM achieves higher distance resolution and reduces mutual interference compared to OFDM [20].

3) DFT-s-OFDM: Compared with the OFDM-based ISAC signal, the DFT-s-OFDM-based ISAC signal has lower PAPR and simple implementation, while retaining the main advantages of OFDM, which allows the receiver to use multiuser joint processing frequency-division multiple access (FDMA) and frequency-domain equalization, while reducing the PAPR of each user, so that it obtains large coverage [74]. In the DFT-s-OFDM signal, data symbols are expanded by DFT block, and then undergo IDFT [75], [76]. In order to avoid ISI

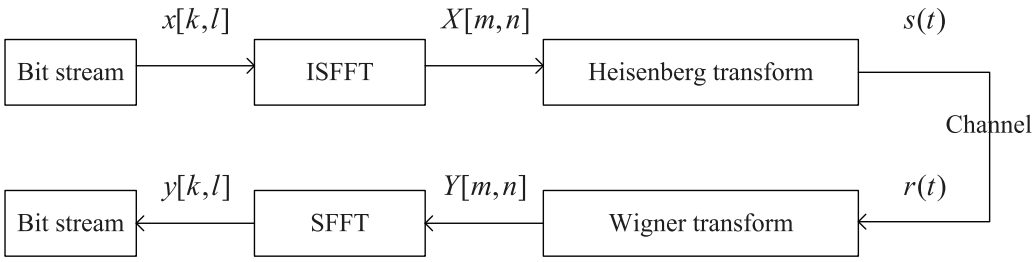

Fig. 7. Signal processing procedure for OTFS signal [30].

caused by the multipath of the channel and allow frequency-domain equalization at the receiver, CP is set to the beginning of the symbol in advance. By changing the size of the DFT block, block-based single carrier signals with different bandwidths are synthesized [77].

Meanwhile, the DFT-s-OFDM ISAC signal is combined with MIMO to achieve high DIR [78]. However, this scheme still generates high PAPR with high-order QAM modulation. Considering the extremely high data rate requirements of 5G-A and 6G, the high-order modulation is commonly applied. Hence, how to maintain the low PAPR and improve the spectral efficiency of DFT-s-OFDM ISAC signal is the challenge of ISAC signal design.

4) OTFS: OTFS is a two-dimensional (2-D) modulation scheme designed in the delay-Doppler domains. The OTFS modulation converts the dual dispersion channel into the delay-Doppler domains using the Heisenberg transform, which is approximately equivalent to a nonfading channel [19], [79]. OTFS modulation has high communication reliability and efficiency in the environment with high mobility [30], because the symbol in a frame experiences nearly the same constant fading in the delay-Doppler domains.

OTFS is an extension of OFDM and is compatible with OFDM by adding a precoding module. The OTFS modulation process is shown in Fig. 7. In the first stage, the symbols in the delay-Doppler domains, namely, $x[k, l]$, are converted into symbols in the time–frequency domains, namely, $X[m, n]$, through inverse symplectic finite Fourier transform (ISFFT). ISFFT is expressed as [30]

$$X[m,n] = \sum_{k=0}^{M-1}\sum_{l=0}^{N-1} x[k,l]\exp\left(j2\pi\left(\frac{mk}{M}-\frac{nl}{N}\right)\right) \quad (11)$$

where m, n and k, l are the indices of the symbols in time–frequency domains and delay-Doppler domains, respectively. N and M are the number of symbols in the delay and Doppler domains, respectively.

Then, the obtained symbols are modulated by Heisenberg transform to form transmitted signal $s(t)$ [30]

$$s(t) = \sum_{\mathrm{n}=0}^{N-1}\sum_{m=0}^{M-1}\left(X[m,n]\exp(j2\pi f_n t)\cdot \mathrm{rect}\left(\frac{t-mT_{\mathrm{sym}}}{T_{\mathrm{sym}}}\right)\right). \quad (12)$$

The signal in the delay-Doppler domains is obtained by calculating the IDFT and Wigner transform of the received signal at the RX. Finally, the window function is applied to improve the channel sparsity in the delay-Doppler domains [80].

OTFS fully reveals the sparsity of wireless channels using delay-Doppler impulse response in terms of communication. Therefore, the number of pilots for channel estimation is reduced, which improves the efficiency of channel estimation, especially for the fading channel with large Doppler frequency shift. Therefore, OTFS is crucial for communication in a highly mobile environment [80].

In terms of radar sensing, OTFS is a fully digitally modulated signal. Gaudio et al. studied the radar sensing performance of OTFS, OFDM, and FMCW. OTFS and OFDM achieve the same sensing performance as FMCW while transmitting at high DIR [79]. Compared with OFDM, OTFS requires a shorter CP and achieves longer sensing distance and faster target tracking rate. Moreover, OTFS is ICI-free, which enables large Doppler frequency shift estimation and detects target with high velocity [80].

OTFS-based ISAC signal is first proposed in [81]. TX transmits signals to RX according to the mobility state of RX, which is obtained by echo signal, to reduce the adverse effects of the channel. The RX demodulates the communication data directly without channel estimation. In other words, the entire OTFS frame is used for communication without setting the pilot used for channel estimation.

III. ISAC Signal Processing

The main radar signal processing methods for ISAC signals are divided into three categories, as shown in Fig. 8, i.e., channel information matrix method, spectrum lines estimator method, and super-resolution method. The channel information matrix method obtains sensing information through constructing a channel information matrix, including 2-D FFT method, cyclic correlation (CC) method, and Bartlett method. The representative method of spectrum lines estimator method is Prony's method. The super-resolution method estimates the distance and velocity of the target by decomposing the received signal into a noise subspace and a signal subspace, including multiple signal classification (MUSIC) method, estimating signal parameter via rotational invariance techniques (ESPRIT) method, and minimum variance distortionless response (MVDR) method.

In 2011, Sturm et al. [90] proposed a radar signal processing algorithm applying 2-D FFT to the received modulation symbol matrix, which simplifies radar signal processing. In order to improve the sensing accuracy and improve the anti-noise capability with low SNR, the CC method and Bartlett's method are proposed, respectively [83], [84]. The CC method is also applicable to ISAC signals using OTFS.

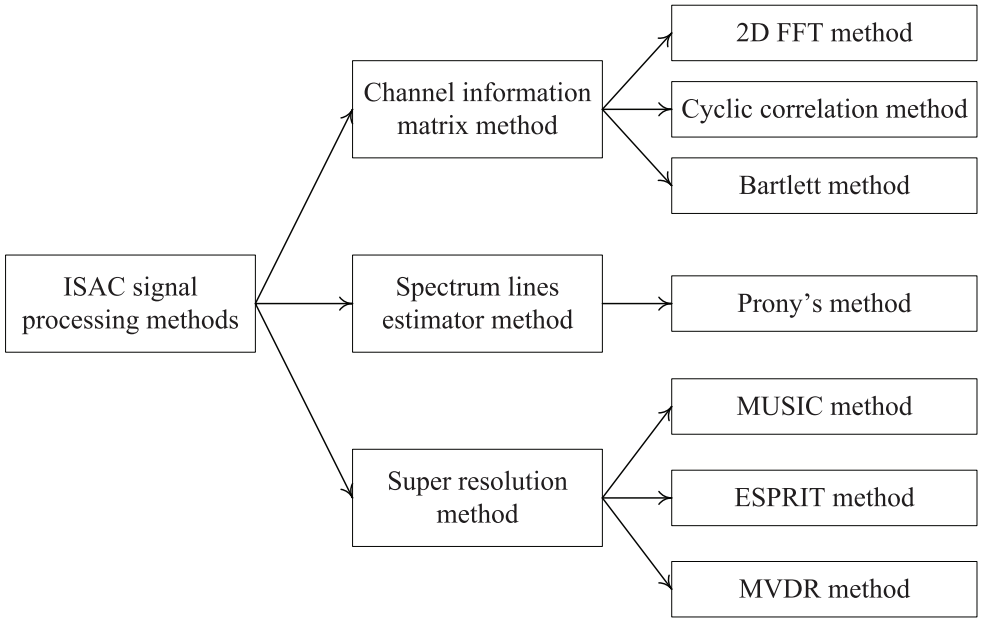

Fig. 8. ISAC signal processing methods.

Prony's method is proposed in 1795 [85]. The sample space is obtained by oversampling the symbols of the OFDM signal. Then, the sensing information, such as distance and velocity, is obtained by solving the differential equation. Schmidt [86] proposed the MUSIC method in 1986. First, the signals received at the antenna array are decomposed into signal subspace and noise subspace through singular value decomposition (SVD). Then, the sensing information is obtained by eigenvalue estimation. In 1986, Roy et al. proposed the ESPRIT method, which applies the shift-invariant structure in the cisoids signal subspace. Besides, the sensing information is estimated by subspace decomposition and generalized eigenvalue calculation [87]. The MVDR method is proposed by Capon in 1969, which has lower computational complexity than that of MUSIC and ESPRIT [88]. In the following sections, these radar signal processing algorithms are reviewed.

A. Performance Metrics of ISAC Signal Processing

This section summarizes the performance metrics of ISAC signal processing, which are used to evaluate the performance of ISAC signal processing in various scenarios.

1) *Computational Complexity:* Computational complexity mainly refers to the time consumption of ISAC signal processing, which is crucial for ISAC signal processing.
2) *Accuracy:* The accuracy reveals the difference between the sensing result and the real value.
3) *Root Mean Square Error (RMSE):* RMSE shows the error of ISAC signal processing algorithm. Since SNR affects the sensing results, RMSE also reveals the anti-noise performance of the ISAC signal processing algorithm.
4) *Cramer–Rao Lower Bound (CRLB):* CRLB is obtained by calculating the likelihood function of the observation value and the Fisher information matrix. CRLB reveals the accuracy of radar sensing [89].

B. Channel Information Matrix Method

1) 2-D FFT Method: The 2-D FFT method directly processes the transmitted and received modulation symbols, rather than operating on the received signals. This approach exploits the time–frequency structure of the OFDM signal and has low complexity [90]. The transmitted OFDM signal is written as

$$s(t) = \sum_{m=0}^{M-1}\sum_{n=0}^{N-1}\left(\mathbf{s}_{T_x}(mN+n) \cdot e^{j2\pi f_n t}\text{rect}\left(\frac{t-mT_{\text{sym}}}{T_{\text{sym}}}\right)\right) \tag{13}$$

where $\mathbf{s}_{T_x}$ is the communication modulation symbol sequence

$$\mathbf{s}_{R_x}(mN+n) = \mathbf{H}(m,n)\mathbf{s}_{Tx}(mN+n) \cdot e^{-j2\pi f_n \frac{2R_r}{c}} e^{j2\pi m T_{\text{sym}} f_{d,r}} \tag{14}$$

where $\mathbf{s}_{R_x}$ is the communication symbols demodulated at RX, $\mathbf{H}$ represents the channel matrix, R_r stands for the distance of target, and $f_{d,r}$ represents the Doppler frequency shift. c is the speed of light propagation.

With the known phase shift of the nth subcarrier eliminated, the channel information matrix $\mathbf{s}_g$ is obtained as

$$\mathbf{s}_g(m,n) = \frac{\mathbf{s}_{R_x}(mN+n)}{\mathbf{s}_{T_x}(mN+n)} = \mathbf{H}(m,n)\left(\bar{\mathbf{k}}_r \otimes \bar{\mathbf{k}}_d\right)_{m,n} \tag{15}$$

with $\otimes$ referring to the Kronecker product. The terms $\bar{\mathbf{k}}_r$ and $\bar{\mathbf{k}}_d$ are as follows [90]:

$$\bar{\mathbf{k}}_r = \left[e^{-j2\pi f_1 \frac{2R_r}{c}}, e^{-j2\pi f_2 \frac{2R_r}{c}}, \ldots, e^{-j2\pi f_n \frac{2R_r}{c}}\right]^T \tag{16}$$

$$\bar{\mathbf{k}}_d = \left[1, e^{j2\pi T_{\text{sym}} f_{d,r}}, \ldots, e^{j2\pi (M-1) T_{\text{sym}} f_{d,r}}\right]. \tag{17}$$

The Doppler frequency shift $f_{d,r}$ and the distance R_r are obtained by DFT transform for each row and IDFT transform for each column of the channel information matrix $\mathbf{s}_g$.

Denoting the peak index of DFT on the nth row of $\mathbf{s}_g$ as $\text{ind}_{s,n}$, the velocity of target v is derived using [90]

$$\begin{aligned} \text{ind}_{s,n} &= \lfloor f_{d,r} T_{\text{sym}} M \rfloor \\ f_{d,r} &= \frac{2vf_c}{c} \end{aligned} \tag{18}$$

where $\lfloor\rfloor$ is the floor function, and f_c is the carrier frequency.

Similarly, denoting the peak index of IDFT on the mth column of $\mathbf{s}_g$ as $\text{ind}_{s,m}$, the distance R_r is derived using [90]

$$\text{ind}_{s,m} = \left\lfloor \frac{2R_r B}{c} \right\rfloor \tag{19}$$

where B is the bandwidth of the ISAC signal.

2) Cyclic Correlation Method: The signal processing method based on correlation method adopts a virtual CP (VCP) according to the sampling points [83]. The maximum detection distance is related to the length of VCP. Therefore, the maximum detection distance is no longer limited by CP. The number of subcarriers and symbols in ISAC signal influence the sensing performance of the 2-D FFT method. However, these parameters are limited by existing communication standards and cannot be dynamically set according to the sensing requirements. Meanwhile, compared with the 2-D FFT method, the CC method is more suitable for processing OTFS-based ISAC signals, where the communication symbols modulated on subcarriers may be 0. In this case, if the 2-D FFT is applied, the sampling value at the RX contains noise. Direct division leads to noise amplification that affects the accuracy of distance and velocity estimation [83].

The CC method samples the echo signal and transmitted signal in the time domain, divides the samples into multiple continuous sub-blocks, then generates the channel information matrix by calculating the correlation between the samples of the echo signal and the samples of the transmitted signal. The estimation results of distance and velocity are obtained by processing the channel information matrix. The essential difference between the CC method and the 2-D FFT method is the approach of grouping sample points. At the RX, the sampling points are grouped in the time domain in the CC method instead of the grouping of sampling points in time–frequency domains in the 2-D FFT method. The channel information matrix in the CC method is obtained by multiplying the values of grouped sampling points by the conjugate of the values of sampling points at the TX. With the obtained channel information matrix, the distance and velocity of the target are obtained using maximum likelihood (ML) and discrete Fourier transform (DFT) methods, respectively [91].

3) Bartlett's Method: The sensing accuracy of the 2-D FFT method varies with the number of FFT points, falling to achieve stable results. According to the correlation of variance, Bartlett divides the signal sequence into several groups and calculates the power spectrum function of each group [92]. This method not only obtains stable and accurates sensing results but also effectively mitigates the impact of noise on sensing results [93].

Using the channel information matrix $\mathbf{s}_g$, Bartlett's method obtains the column vector yielding distance and the row vector yielding velocity. The obtained vector is divided into several groups, and the power spectrum function of each group is calculated. Then, the power spectrum function of each group is accumulated and averaged to obtain the average periodic graph. The peak is searched according to the average periodogram. Then, the distance and velocity of target are calculated [84].

C. Spectrum Lines Estimator Method

In 1795, Prony proposed a method using a set of linear combinations of exponential functions to fit uniformly sampled data. The sensing information is obtained by solving difference equations. In the presence of noise, this method transforms the parameter estimation into an optimization problem to improve the sensing resolution. The steps of Prony's method are provided as follows [85].

Step 1: Data vector is obtained by adopting a sampling scheme. Assuming that the kth sampling symbol at the RX is expressed as

$$s_k = \sum_{n=0}^{N-1} a_n \left(e^{j2\pi (f_n + \sigma_k)\Delta t} \right)^{k-1} + \omega_k \tag{20}$$

where Δt is the sampling interval N is number of subcarriers, a_n is the modulation symbol, σ_k is the frequency error during sampling, and ω_k is the AWGN. The purpose of this step is to estimate $e^{j2\pi (f_n+\sigma_k)\Delta t}$ from the sampled value.

Step 2: The characteristic equations of the linear difference equations are constructed as

$$s_k + \sum_{i=1}^{N} b_i s_{k-i} = \omega(k) + \sum_{i=1}^{N} b_i \omega(k-i) \; k = 1, 2, \ldots, N \tag{21}$$

where b_i is the coefficient that makes the sampling s_k satisfy Yule-Walker equation.

Step 3: Characteristic roots are derived according to the characteristic equations.

Step 4: Doppler frequency shift and delay of the signal are derived according to the characteristic roots [85].

Prony's method uses a set of sampled values to obtain the sensing information. However, Prony's method is affected by the sampling interval and noise. The total least squares-SVD (TLS-SVD) algorithm is used to reduce the amount of calculation and overcome the impact of noise on ISAC signal processing [85]. The characteristic roots of the signal are obtained according to the singular value. Then, Doppler frequency shift and delay are derived using the characteristic roots.

D. Super-Resolution Method

The accuracy of 2-D FFT and CC methods is limited by the sampling rate. Super-resolution methods effectively overcome the limitations of the sampling rate and provide higher estimation accuracy and resolution compared with the channel information matrix method and spectrum lines estimator method. The MUSIC method comprehensively has the best accuracy among the super-resolution methods with high

TABLE VII
PERFORMANCE COMPARISON OF SUPER-RESOLUTION METHODS

Super resolution methods	Computational complexity	Accuracy	Resolution
MUSIC	High	High	Medium
ESPRIT	Medium	Medium	High
MVDR	Low	Low	Low

computational complexity. The accuracy and computational complexity of the ESPRIT method are both the medium [94]. Although the implementation of the MVDR method is simple, it has low resolution and accuracy. The performance comparison among the super-resolution methods in terms of computational complexity, accuracy, and resolution is shown in Table VII.

1) MUSIC Method: The MUSIC method adopts the matrix eigenspace decomposition, which provides an asymptotically unbiased estimation of a) the number of incident wavefronts; b) the direction of arrival (DoA) and distance of the target; c) the strength and cross-correlation between the incident signals; and d) the strength of noise and interference. The steps of the MUSIC method are provided as follows [86].

Step 1: The signal received at the antenna array composing of M antenna elements is the combination of echo signals and noise. It is represented as a vector $\mathbf{X}$

$$\mathbf{X} = \mathbf{AF} + \mathbf{W} \tag{22}$$

where $\mathbf{A}$ is a matrix of the phase difference of the echo signal on the antenna elements due to the delay of signal propagation, $\mathbf{F}$ represents the sampling value of the echo signals on the reference antenna array, and $\mathbf{W}$ represents the noise received by the antenna array.

Step 2: The signal subspace and noise subspace are obtained by calculating the autocorrelation matrix $\mathbf{R_{XX}}$ of $\mathbf{X}$.

Step 3: The spatial spectrum $P_{MU}(\theta)$ is obtained by constructing an orthogonal relation equation according to the orthogonal relation between the signal subspace and the noise subspace.

Step 4: Sensing information, such as DoA, distance, velocity, etc., is obtained by searching the peak of the spatial spectrum function.

As shown in Fig. 9, when estimating DoA, the echo signals received by different antenna elements are used to construct spatial spectrum function. When estimating distance and velocity, the channel information matrix is constructed as the method in Section III-B1. Then, the phase differences of subcarriers and OFDM symbols are applied to estimate the distance and velocity of target, respectively. Specifically, the spatial spectrum functions are constructed using the row vector and column vector of the channel information matrix by undergoing the above steps. Then, the distance and velocity of target are estimated by searching the peaks of these spatial spectrum functions. The MUSIC method provides parameter estimation close to CRLB. Simulation results in [86] demonstrate that the MUSIC method estimates the DoAs of multiple targets

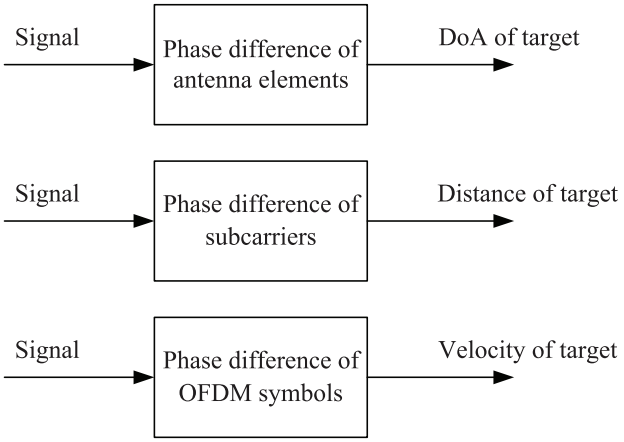

Fig. 9. MUSIC method estimating DoA, distance, and velocity of the target.

with higher accuracy than ML [95] and maximum entropy (ME) [96] methods.

2) ESPRIT Method: In order to solve the challenge of blind synchronization of OFDM signal in mobile communication systems, Ufuk et al. [82] proposed ESPRIT. This method exploits the structure information of OFDM signals to estimate sensing information. Compared with the MUSIC method, the ESPRIT method provides the same resolution with lower complexity. Simulation results show that the ESPRIT method is superior to the MUSIC method in terms of complexity [82].

Similar to the MUSIC method, the ESPRIT method exploits the signal and noise to generate asymptotically accurate estimation of distance and velocity. The ESPRIT method has the following advantages.

a) The ESPRIT method does not require the knowledge of antenna patterns.
b) The complexity of the ESPRIT method is much lower than the MUSIC method because it does not need the search procedure inherent in the MUSIC algorithm, namely, Step 4 in the MUSIC algorithm.
c) The ESPRIT method simultaneously estimates the number of sources and their DoAs [82].

ESPRIT exploits the rotational invariance signal subspace. The steps of the ESPRIT method are provided as follows [82].

Step 1: The K samples of the received signal are given by

$$\mathbf{X}[k] = \sum_{n=1}^{N} a_n e^{j2\pi f_n t} + \omega[k], k = 0, 1, \ldots, K-1 \tag{23}$$

where a_n is the symbol modulated on the nth subcarrier, and $\omega[k]$ is the AWGN.

Step 2: In order to exploit the deterministic nature of the cisoids, $\mathbf{X} = [\mathbf{X}[0], \mathbf{X}[1], \ldots, \mathbf{X}[K-2]]$ and $\mathbf{Y} =$

$[\mathbf{X}[1], \mathbf{X}[2], \ldots, \mathbf{X}[K-1]]$ are constructed. The autocorrelation matrix $\mathbf{R_{XX}}$ and cross-correlation matrix $\mathbf{R_{XY}}$ are derived.

Step 3: Calculating the eigendecomposition of autocorrelation matrix $\mathbf{R_{XX}}$, the minimum eigenvalue is the variance of noise σ^2.

Step 4: The generalized eigenvalue matrices $\mathbf{C_{XX}}$ and $\mathbf{C_{XY}}$ are calculated using the variance of noise as follows:

$$\mathbf{C_{XX}} = \mathbf{R_{XX}} - \sigma^2 \mathbf{I} \tag{24}$$

$$\mathbf{C_{XY}} = \mathbf{R_{XY}} - \sigma^2 \mathbf{Z} \tag{25}$$

where $\mathbf{I}$ is the identity matrix, $\mathbf{Z}$ is given by

$$\mathbf{Z} = \begin{bmatrix} 0 & . & . & . & 0 & 1 \\ 0 & . & . & . & 1 & 0 \\ . & & & . & . & . \\ . & & . & & . & . \\ . & . & & & . & . \\ 1 & . & . & . & 0 & 0 \end{bmatrix}. \tag{26}$$

When estimating DoA, the received signals of different antenna array elements are used to construct the covariance matrices and the generalized eigenvalue matrices, which are applied to calculate the subspace rotation operator. The eigenvalue of subspace rotation operator yields DoA of target [87]. When estimating the distance and velocity of the target, the channel information matrix is constructed as the method in Section III-B1. The covariance matrices and the generalized eigenvalue matrices are obtained using the row vector and column vector of the channel information matrix by undergoing the above steps. Then, the subspace rotation operators for distance and velocity estimation are constructed, whose eigenvalues yield the distance and velocity of target.

3) MVDR Method: Capon proposed the MVDR method in 1969. Compared with MUSIC and ESPRIT methods, the MVDR method has the advantages of easy implementation and minimizing the power of noise and interference, thereby mitigating their impact on sensing performance. MUSIC and ESPRIT methods have better sensing performance than MVDR method with the same number of sampling points [88].

Similar to MUSIC and ESPRIT methods, the MVDR method first constructs channel information matrix. The column and row vectors of the channel information matrix are weighted and summed to obtain the frequency response vectors projected into the delay and Doppler domains, respectively. By using frequency response vectors, the autocorrelation matrices are constructed. The spatial spectrum functions are then constructed according to the autocorrelation matrices and the peak indices of the spatial spectrum functions are obtained, yielding the estimation of distance and velocity of target [88].

E. Signal Processing for OFDM-Based ISAC Signals

According to the above algorithms, 2-D FFT estimates the distance and velocity of target with low complexity. Therefore, the 2-D FFT method is widely applied to process most OFDM-based ISAC signals. This section briefly reviews the signal processing methods for the OFDM-based ISAC signals.

1) ISAC Signal Combining OFDM and LFM: The modulation symbol is recovered from the received signal by removing CP and undergoing FFT. The echo signal is expressed as

$$r(t) = \sum_{n=0}^{N-1} \sum_{m=0}^{M-1} \Bigg(\mathbf{H}(n,m) d(mN+n) \mathrm{e}^{j2\pi f_d t} \mathrm{e}^{j2\pi f_n (t-\tau)} \cdot \mathrm{e}^{j\pi k (t-\tau)^2} \mathrm{rect}\left(\frac{t - mT_{\mathrm{sym}} - \tau}{T_{\mathrm{sym}}} \right) \Bigg) \tag{27}$$

where $\mathbf{H}(n,m)$ is the channel response of the nth subcarrier of the mth symbol, f_d is the Doppler frequency shift, and $\tau = (2R_r/c)$ is the delay [55].

At the RX, the same steps are performed in reverse order to the TX. Because of the existence of CP, the demodulator can capture the signal of a complete symbol period and obtain the starting point of the symbol period, which guarantees that the result of 2-D FFT is correct. When the signal is dechirped, the received modulation symbols are recovered by calculating the FFT of the received baseband signal.

2) ISAC Signal Combining OFDM and Phase Coding: Combining OFDM and phase coding, as given in (7), the received signal with downconversion is obtained as [43]

$$r(t) = \sum_{n=0}^{N-1} \sum_{m=0}^{M-1} \Bigg(\mathbf{H}(n,m) a_{n,m} \mathrm{e}^{j2\pi f_d t} \cdot \mathrm{rect}\left(\frac{t - mt_b - \tau}{t_b} \right) e^{j2\pi f_n (t-\tau)} \Bigg). \tag{28}$$

There are multiple methods of ISAC signal processing. Take 2-D FFT method as an example. The channel information matrix is obtained. Then, the distance and velocity of target are obtained using the 2-D FFT method [43].

3) ISAC Signal Based on Spread Spectrum: Take 2-D FFT method as an example. Before the OFDM modulation of the SS-OFDM signal, the communication symbols are spread by the spread spectrum sequence. Similarly, the received matrix is composed of the transmitted symbols. The received matrix is divided by the transmitted matrix, generating the channel information matrix. The distance and velocity of the target are obtained using the 2-D FFT method [97].

F. Signal Processing for OTFS-Based ISAC Signals

The RX of OTFS signal performs the inverse process of the TX, converting the received signal to the delay-Doppler domains for demodulation [19]. Specifically, the received signal in the time domain is first processed by Wigner transform, and then the symbols in the delay-Doppler domains are obtained by adding a receiving window function and calculating SFFT as shown in Fig. 7.

Gaudio et al. [31] proposed OTFS-based ISAC signal and the corresponding signal processing algorithm. The ML algorithm is applied in radar signal processing and the soft-output detector utilizing channel sparsity in Doppler-delay domains is applied for communication [31]. Then, with the combination of OTFS and MIMO, they further applied ML algorithm in estimating the DoA, distance, and velocity of target. Two steps of coarse and refined parameter estimation are designed to reduce the complexity of ISAC signal processing [98]. Raviteja et al. proposed a matched filter for the distance and

TABLE VIII
ISAC SIGNAL OPTIMIZATION

Category	Optimization method	One-sentence summery
PAPR optimization	Coding method	The coding method is used to design the information sequence to avoid the occurrence of large signals.
	Probability method	PTS and SLM are used to restrain PAPR.
	Tone reservation	Part of LFM signals are used for information transmission, while other LFM signals are used for PAPR suppression.
Interference management	Mutual-interference cancellation	One user's ISAC signal brings interference to another user's reception of the echo of ISAC signal.
	Self-interference cancellation	The signal sent by TX interferes with the echo signal received by RX.
	Interference avoidance	Duplex or multiple access are used to avoid interference between users.
Adaptive signal optimization	Total power constraint	When the maximum power of the signal is determined, the ISAC signal is designed with the best performance.
	Mutual information (MI) constraints	Design adaptive ISAC signals to achieve maximum MI.
	Indoor environment	Adaptive ISAC signals are used to achieve optimal scattering characteristics.
	Pilot structure design	The sensing performance and anti-noise ability of signal are improved by inserting pilot.

velocity estimation of the target. Compared with the CP overhead in OFDM, OTFS requires less overhead. Meanwhile, since OTFS signal has no ICI, it achieves more accurate Doppler frequency shift estimation, achieving more accurate velocity estimation compared with OFDM signal [19].

IV. ISAC SIGNAL OPTIMIZATION

ISAC signal optimization mainly includes three categories, i.e., PAPR optimization, interference management, and adaptive signal optimization, as shown in Table VIII. ISAC signal with high PAPR is easy to enter the nonlinear region of the power amplifier, which leads to signal distortion. Therefore, an effective PAPR reduction scheme is necessary to reduce the PAPR of ISAC signal. The RX will encounter the self-interference from the TX and the mutual interference from other TX, which will degrade the sensing performance. Hence, interference management is essential in ISAC signal optimization. As the application scenarios of the ISAC signal are various, adaptive signal optimization is required, including signal parameter optimization and signal structure optimization. Through signal optimization, ISAC signal adapts to various application scenarios and improves the performance of sensing and communication.

A. PAPR Optimization

High PAPR may cause OOB or in-band distortion of the transmitted OFDM signals [37]. Thus, the OFDM signals require a large linear dynamic range of power amplifiers to avoid distortion. This section reviews the coding method, tone preserving method, and probability method to reduce PAPR.

1) Coding Method: When the OFDM signal has a large amplitude, it may produce a high PAPR. However, this only occurs when the modulation symbols of the OFDM signal form a tightly structured symbol sequence. The coding method generates a signal with low PAPR by coding sequences [99]. The bit stream is processed through the coding sequences to generate a plurality of candidate sequences. The candidate sequences are modulated into symbol sequences. The PAPR of the OFDM signal for each symbol sequence is first calculated, and then the candidate sequences that produce high peak power are discarded. Since some candidate sequences are abandoned, the bit stream needs to be transmitted with long codes. For example, 3-bit information needs to be encoded with 4-bit coding sequences. The coding methods have a large amount of calculation, because it needs to exhaust all the candidate sequences. However, the coding methods are applicable to the case where the coding sequence is short and the number of subcarriers is small. The number of candidate sequences that need to be exhausted will grow rapidly if there are many subcarriers [100].

Take the Golay code as an example. The Golay sequence is a typical code reducing PAPR with strong error correction capability and high sensing performance [101]. Using the Golay sequence, PAPR is reduced to 3 dB [99].

The OFDM signal is a superposition of modulation symbols over all the subcarriers. A self-disarrange block coding method is proposed to reduce PAPR [100]. First, Golay sequences are applied to encode the information bits to obtain an encoded packet. Then, the proposed algorithm generates all arrangements of encoded packets on the OFDM symbol. Finally, the modulation symbol sequence with the lowest PAPR is selected. In addition, the P4 sequence is used to reduce PAPR, and the phase code sequence of the signal is designed by cyclic shift based on the P4 sequence [102].

2) Probability Method: The probability method is an extension of the coding method. The idea of the probability method is to use a sequence set to represent a bit stream of communication information. Then, the sequence with the lowest PAPR is selected from the sequence set and regarded as

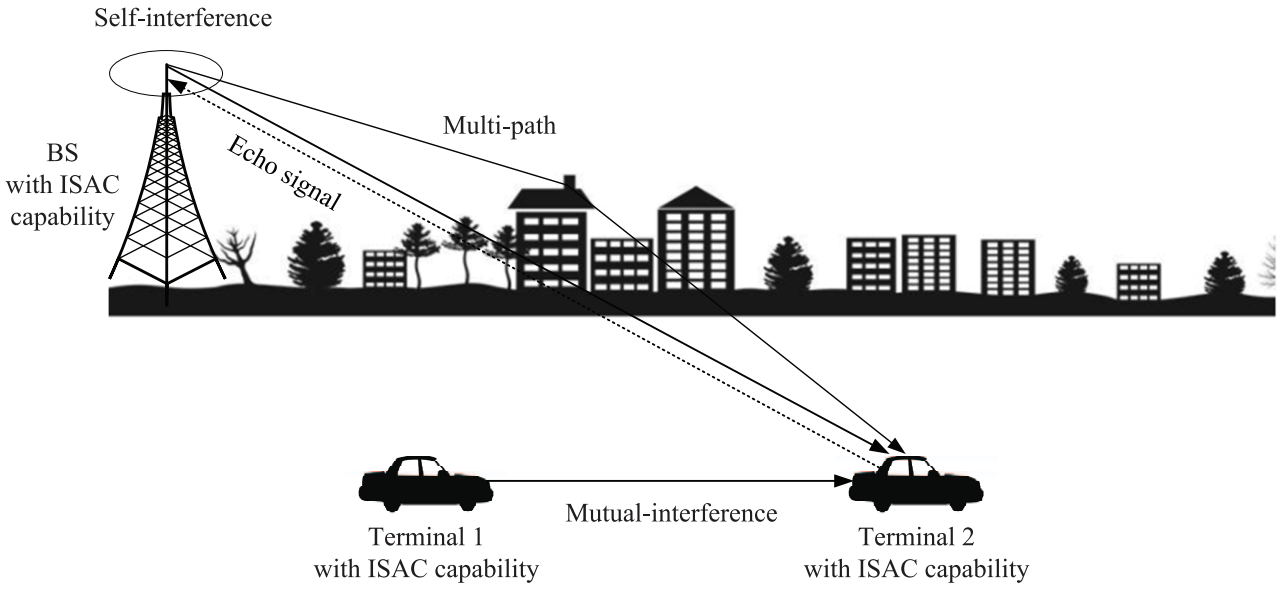

Fig. 10. Multipath and multiuser scenario.

the transmission sequence. Commonly used probability methods mainly include partial transmission sequence (PTS) and selected mapping (SLM) [103].

The PTS divides the modulation symbols into several sub-blocks. Each sub-block is modulated onto fixed subcarriers and adjusted with different phase factors to minimize the PAPR of each sub-block. The ability to reduce PAPR improves as the number of sub-blocks increases [103].

The SLM converts the original modulation symbols into low PAPR symbols. This method generates modulation symbols according to the original modulation symbols created by the TX. Then, the modulation sequence with a low PAPR is selected to transmit, thereby reducing PAPR without distorting the transmitted signal [104].

Both PTS and SLM need to record the side information (SI) indicating the modulation symbols. The RX demodulates the modulation symbols according to the SI index to obtain the communication symbol. The performance of communication and sensing at RX depends on the accuracy of SI [103], [104].

An SLM method without sending SI indices is proposed in [104], where the SI indices are embedded into the modulation sequence to reduce the overhead in the transmitted sequence. In order to reduce PAPR efficiently, a method combining SLM and PTS is proposed in [103]. The modulation symbol sequences first undergo SLM. When the PAPR of the output sequence of the previous step is smaller than a threshold, the sequence is chosen to be modulated on the ISAC signal at TX. Otherwise, the output sequence is further processed using the PTS method. This method reduces the PAPR with low complexity without degrading the performance of communication and sensing.

3) Tone Reservation: The tone reservation method reserves some subcarriers to modulate LFM signals and generate peak canceling signals. Other subcarriers are used to transmit communication signals. This method has low complexity and BER. However, some subcarriers are reserved to reduce PAPR, resulting in the waste of spectrum resources.

In [105], a PAPR reduction method is proposed using the tone reservation method. An orthogonal chirp-division multiplexing (OCDM) signal is composed of N orthogonal LFM signals and OFDM signals. Compared with the classical tone reservation method, this scheme requires fewer peak cancellation signals to reduce PAPR. The performance of PAPR reduction improves as the number of peak cancellation signals increases. The tone-preserving method is combined with the SLM method by first performing the SLM method, and then performing the tone preserving method, which reduces the PAPR more effectively than the tone reservation method [106].

B. Interference Management

Interference is one of the nonnegligible factors that restrict the performance of the ISAC system. ISAC interference mainly consists of mutual interference and self-interference. For the ISAC system, since the echo signal usually returns to the RX before the transmission is completed, the transmission will interfere with the echo signal, which causes self-interference. When the ISAC system is applied in the multipath and multiuser scenario, the ISAC signal transmitted by one user may cause interference to other users, resulting in mutual interference. If there is strong mutual interference and self-interference, as shown in Fig. 10, the sensing performance of the ISAC system will be severely degraded, failing to correctly identify targets within its detection distance.

1) Mutual-Interference Cancellation: Typical mutual-interference cancellation algorithms consist of serial interference cancellation [107] and selective interference cancellation [16], [108], [109].

a) Serial interference cancellation: The core method of the serial interference cancellation is to demodulate the received ISAC signal. Then, the reconstructed interference signal from the received signal is subtracted [107]. The Schmidl and Cox (S&C) algorithm is first used to detect interference signals through amplitude attenuation and phase rotation. Then, starting from the identified interference signal with the

maximum power, the interference signal is decoded successively. Finally, in order to reconstruct the signal, it is necessary to remodulate the correct demodulation interference signal, and add the amplitude attenuation, phase rotation, frequency offset, and delay. Then, the reconstructed interference signal is subtracted from the original ISAC echo signal to eliminate the interference.

One of the challenges of serial interference cancellation is that the amplitude attenuation and phase rotation of the interference signals with the same delay cannot be detected by correlation. It is shown in [107] that when the power difference between the identified interference signal and other received signals is smaller than 15 dB, the frequency offset may be misestimated by the S&C algorithm. Moreover, the residual frequency offset in the estimation process will have a cumulative effect on the subsequent signal subtraction [16], [108], [109].

b) Selective interference cancellation: Different from serial interference cancellation, only the strongest identified interference will be reconstructed for selective interference cancellation [108]. Selective interference cancellation only needs one cycle processing, and it does not leave ambiguous dots, which will not be mistaken as a target.

However, the performance of the two interference cancellation algorithms largely depends on the correct frequency offset estimation. Minor errors in frequency offset estimation may lead to incorrect signal reconstruction.

2) Self-Interference Cancellation: In addition to mutual-interference, self-interference is also the main factor impacting the performance of the ISAC system. The self-interference may be much stronger than the echo signal, since the TX is close to the RX [110]. Although the radar RX knows the transmitted signal, the channel is random, making self-interference cancellation challenging.

The adaptive interference cancellation method proposed in [111] generates the cancellation signal with the opposite phase and equal amplitude to the self-interference signal, and then adds it to the received signal to cancel the self-interference. In [110], instead of using a direct interference cancellation scheme, the self-interference channel between transmitting and receiving antennas is estimated to eliminate the self-interference and realize full-duplex operation, which is suitable for moving target detection. In [112], the self-interference of an omnidirectional antenna is considered, and the least-squares matching pursuit (LSMP) algorithm was used to search all targets iteratively. Barneto et al. [11], [113] indicated that promoting sufficient TX-RX isolation is a critical issue to be considered. In order to achieve adequate TX-RX isolation, appropriately customized RF and digital cancellation solutions are designed in [11] to cancel the self-interference without suppressing the echo signals of actual targets.

3) Interference Avoidance: Another solution to interference management is interference avoidance, which adopts the schemes such as duplex or multiple access to avoid the interference, such that there is no need to apply complex interference cancellation schemes.

a) Mutual-interference avoidance: For multipath and multiuser scenarios shown in Fig. 10, a multiple access scheme is applied to distinguish different ISAC users, so as to avoid mutual interference. Common multiple access methods include time-division multiple access (TDMA), code-division multiple access (CDMA), orthogonal frequency division multiple access (OFDMA), and carrier sense multiple access (CSMA), which are applied to avoid mutual interference in the ISAC system.

The principle of TDMA is that different ISAC users transceive signals within the specified time slots, avoiding the interference. In [114], the TDMA is applied for channel allocation among multiple radars to achieve the required channel isolation level.

With CDMA, ISAC users are assigned with orthogonal code sequences for channel separation to avoid mutual interference. One method for mutual-interference avoidance is to combine CDMA with DSSS techniques to design ISAC signal. In [50], a new ISAC signal based on multicarrier-direct sequence-CDMA (MC-DS-CDMA) is proposed. The radar subsystem uses spread spectrum codes with ideal autocorrelation and cross-correlation characteristics to estimate distance and uses scrambling codes to distinguish radar and communication signals. In [115], an ISAC signal combining radar sensing with DSSS communication is proposed, which reduces the interference between multiple users. Another method is to adopt a signal processing scheme to suppress interference. In [97], a code-division-OFDM (CD-OFDM) ISAC system is proposed. The corresponding serial interference cancellation-based signal processing method is proposed to suppress the mutual interference, which achieves code-division gain to suppress the interference between radar echo signal and communication signal.

With OFDMA, each user is assigned a subset of subcarriers, and multiple users transmit simultaneously. In [116], the concept of OFDMA radar is proposed, and a subset of subcarriers is allocated to each radar task so that the radar performs multiple tasks at the same time. The OFDMA radar has the advantages of high sensing accuracy, strong anti-clutter and anti-interference ability, and high spectrum efficiency. In [117], based on OFDMA, the concept of interference-aware power allocation is proposed to improve sensing ability and clutter suppression. The subcarriers overly affected by clutter will be dropped.

CSMA is a distributed multiple access method to avoid transmission conflict. In [118], an FMCW radar based on CSMA is proposed, which simultaneously avoids both wideband and narrowband interferences causing miss detection and false alarm. In [119], a novel concept of packet-based FMCW radar using CSMA is proposed to reduce the probability of narrowband interference causing false alarm of ghost target [120].

b) Self-interference avoidance: Self-interference is the main challenge of a full-duplex ISAC system, which will degrade the sensing performance. The performance of self-interference cancellation under the full-duplex assumption is limited and has high computational complexity in the digital domain. Therefore, self-interference avoidance is essential to improve the sensing performance with imperfect self-interference cancellation. In [121], the Golay sequence in

the preamble is applied to reduce self-interference in short-distance sensing. In addition, for long-distance sensing, a pilot signal is designed, where the OFDM symbols without self-interference at the end of OFDM data frame are used to achieve accurate distance estimation. This method does not need self-interference cancellation in the digital domain, which reduces the computational complexity. In [122], a factor-graph approach is proposed for joint channel estimation, self-interference mitigation, and decoding, which is suitable for OFDM-based self-interference-limited transmissions.

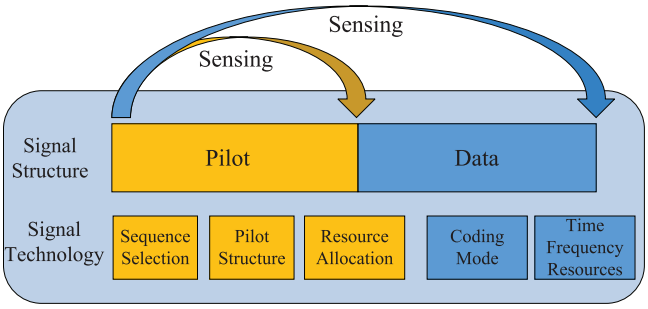

Fig. 11. ISAC signal structure.

C. Adaptive Signal Optimization

According to the domains of the decision variables, different ISAC signal parameter optimization algorithms are proposed. Adaptive signal optimization methods are proposed for various scenarios, including ISAC signal parameter optimization and ISAC signal structure optimization. When optimizing the parameters of ISAC signal, the objective functions and constraints need to be designed according to the requirements of scenarios, including sensing MI, DIR, PAPR, transmit power, etc. ISAC signal optimization faces the tradeoff between the performance of sensing and communication, which is a challenge of ISAC signal optimization [123]. According to the decision variables, different ISAC signal parameter optimization algorithms are proposed.

1) ISAC Signal Parameter Optimization: The parameters of ISAC signal in space–time–frequency domains need to be optimized to satisfy the requirements of communication and sensing in various application scenarios.

a) Parameter optimization in space domain: The beamforming and precoding methods have been proposed for the ISAC signal optimization in the space domain. In [68], the impact of random communication signal on radar peak sidelobe level (PSL) is reduced by selecting the signal with high PSL to detect weak targets accurately. The transmit waveform matrix is optimized for designing the radar beam pattern under the constraints of transmit power and signal-to-interference plus noise ratio (SINR) in [124]. The CRLB of sensing channel estimation is minimized under the constraint of SINR for each user [125]. In [126], a low-complexity minimum beam pattern gain maximization method is proposed to match the beam pattern and maximize the minimum weighted beam pattern gain.

b) Parameter optimization in time–frequency domains: In terms of the ISAC signal optimization in time–frequency domains, existing works applied the sensing and communication MI and CRLB to optimize the ISAC signal.

Several literature take sensing MI as the objective function of the ISAC signal optimization. For example, the sensing MI is maximized under the constraints of DIR and subcarrier power ratio to improve the performance of ISAC systems in [127]. The weighted sum of sensing MI and communication MI is maximized under the total power constraint to obtain a closed-form solution for optimal power allocation of ISAC signals [21], [38].

Besides sensing and communication MI, other performance metrics are adopted as the objective functions. Chen et al. [128] maximized the detection probability of radar sensing under the constraints of the total transmit power and DIR. In point-to-point communication scenarios, the power of the ISAC signals is optimally allocated under the constraints of pulse compression sidelobe and communication data rate in [129]. The proposed method in [129] outperforms traditional windowing and waterfilling techniques under severe channel fading conditions. In [130], an adaptive ISAC signal optimization model with the ME, SNR, and DIR is established under the constraint of total power. To achieve a balanced tradeoff between sensing and communication, the CRLB of sensing channel estimation is minimized to enhance the sensing accuracy and channel capacity under the constraint of total transmit power [131]. To solve the optimization model, they proposed two signal optimization methods, namely, the weighted optimization ISAC signal design and the Pareto-optimal ISAC signal design method.

2) ISAC Signal Structure Optimization: The signal structure is divided into the pilot and data parts, as shown in Fig. 11. The pilot signal is known in the modulation domain and is normally inserted in the OFDM signal for synchronization and channel estimation [132]. The pilot signal has the advantages of high power, excellent sensing performance, and strong anti-interference capability, which has the potential to be applied in radar sensing [133]. The performance of the ISAC signal is improved by optimizing the pilot signal structure. Pilot sequences with ideal autocorrelation characteristics are used to improve the performance of radar sensing. In addition, the structure and resource allocation of the pilot also affect the performance of radar sensing.

In terms of sequence selection, sequences with ideal autocorrelation characteristics and good cross-correlation characteristics should be selected. In [134], the preamble composed of Golay sequence of 802.11ad is applied to radar sensing because of its good autocorrelation properties. In [135], the Zadoff–Chu sequence is used for radar processing because of its good correlation performance, which reduces the impact of phase between adjacent pulses. In [133], the performance of 5G reference signals, including positioning reference signal (PRS), demodulation reference signal (DMRS), channel state information-reference signal (CSI-RS), and synchronization signal (SS), is verified and it is proved that PRS has advantages in radar sensing. Further, the concept of sensing reference signal is proposed by exploiting the existing reference signal in radar sensing, which is specifically suitable to 5G-A.

In terms of the pilot structure, due to the 2-D time–frequency properties of OFDM signals, the pilot signals are

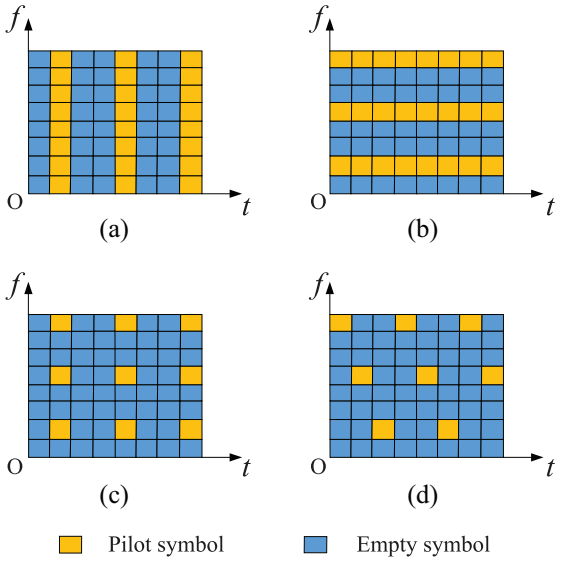

Fig. 12. Main pilot structures. (a) Block pilot. (b) Comb pilot. (c) Rectangle discrete pilot. (d) Rhombus discrete pilot.

inserted in the 2-D resource blocks. There are three common pilot structures as shown in Fig. 12. Block pilots are distributed continuously in the frequency domain and discretely in the time domain, which are suitable for frequency-selective fading channels. The comb pilots are continuously distributed in time domain and discretely in frequency domain. Comb pilots are suitable for time-selective fading channels. Discrete pilots are discretely inserted in both the time and frequency domains, which saves time–frequency resources and significantly improves spectrum efficiency [136], [137].

The comb pilot structure is adopted in [136], where the pilot sequence is Barker code and the radar signal processing method combining matched filter and 2-D Fourier transform is applied. The distance resolution of 0.1 m and velocity resolution of 0.58 m/s are realized. In [137], an OFDM-MIMO ISAC system using a superimposed pilot is proposed. Compared with comb pilot and block pilot, the superimposed pilot has the advantages of comb pilots in velocity estimation and block pilots in distance estimation, which is suitable for frequency-selective and fast fading channels.

In terms of resource allocation, the subcarrier allocation between the data and pilot is optimized to maximize the sensing accuracy and channel capacity [136]. In [138], the dynamic change of the number of pilot subcarriers is used for radar detection at different distances, which realizes short-range radar (SRR), medium-range radar (MRR), and long-range radar (LRR). A full-duplex ISAC system is proposed in [139], where the pilot overhead is used for channel estimation and radar sensing, and the sum data rate is optimized according to the pilot overhead and power.

In addition, as shown in Fig. 11, the autocorrelation of the data part is improved by utilizing phase coding to enhance the sensing performance [101]. Radar sensing with both pilot and data achieving high sensing performance is the future trend in ISAC signal design and optimization.

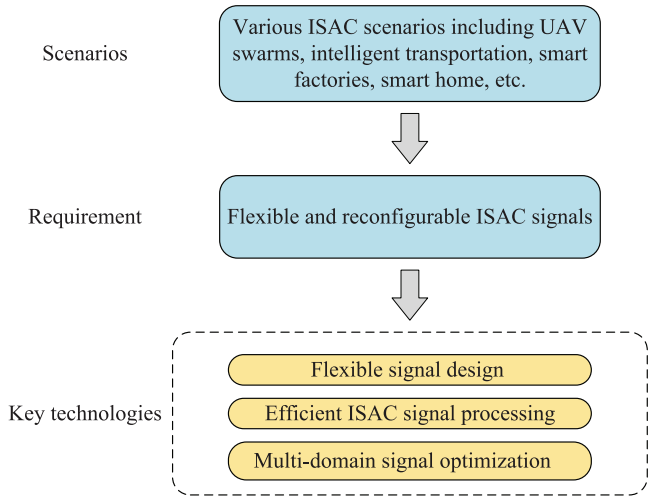

Fig. 13. Future research trends of ISAC signals.

V. Future Trends

The application scenarios of ISAC systems are various. As shown in Fig. 1, typical scenarios include UAV swarm, intelligent transportation, smart factory, smart home, etc. Therefore, the ISAC signals need to be flexible and reconfigurable, adapting to diverse scenarios. As shown in Fig. 13, this section provides the future research trends of ISAC signals for various application scenarios, including signal design, signal processing, and signal optimization, to realize the goal of flexible and reconfigurable ISAC signals.

A. ISAC Signal Design

ISAC signal design mainly includes waveform design, frame structure design, and transmission mode design. Academics continue to propose new waveforms for 5G-A and 6G. It is crucial to select the appropriate waveform for ISAC through performance evaluation. It is necessary to optimize the frame structure to improve the efficiency of communication and sensing. In terms of transmission mode, the duplex method is still an open problem.

1) Waveform Design: OFDM is the mainstream modulation technology in mobile communication systems. However, various waveforms, such as FBMC, GFDM, and OTFS, are proposed for the next-generation mobile communication systems, which are the further trends of modulation technology. Considering the high DIR and sensing accuracy of the signals on the THz spectrum bands, the ISAC signals on THz bands have great advantages in improving the performance of sensing and communication. It is noted that the candidate ISAC signals on THz bands include DFT-s-OFDM, single carrier-frequency domain equalization (SC-FDE), etc.

As part of the Internet of Things (IoT) applications, it is expected that ISAC technology will be required not only on the base station (BS) side for sensing the surrounding environment, such as intelligent transportation, but also on the terminal side in various IoT scenarios, such as smart home.

Specific requirements need to be considered in the modulation technology. For example, low sidelobe, high reliability [140], and multiuser interference [141]. In addition, due

to the different requirements of communication and sensing, it is necessary to balance communication and sensing when designing the ISAC signal.

2) Frame Structure: Existing ISAC signals generally adopt the frame structure specified by the standards, such as 3GPP 5G NR and IEEE 802.11. In complex scenarios, the fixed frame structure cannot perfectly adapt to differentiated requirements. Hence, the frame structure design of ISAC signals should be flexible and reconfigurable to adapt to various scenarios. The existing ISAC signals generally apply pilots to realize the sensing function, which will not affect the communication function. When more resources are allocated to the pilot, the sensing performance will be improved, and the communication performance will be degraded. There are some studies on the flexible design of the ISAC frame structure. In [136], the pilot and data subcarriers are optimally allocated to improve the performance of sensing and communication. The pilot-based ISAC signal in [142] flexibly allocate the pilots to achieve long-distance sensing [142]. In the future, joint optimization of the parameters in space–time–frequency domains adapts to various scenarios and realizes flexible and reconfigurable ISAC signals.

3) Transmission Mode: The transmission modes of communication include full-duplex and half-duplex. The majority of ISAC systems adopt half-duplex mode. Xiao and Zeng [143] proposed a full-duplex ISAC scheme, which uses the waiting time of traditional pulse radar to transmit communication signals. Compared with the traditional ISAC signal, this scheme improves the DIR and solves the problem of blind detection. However, the transmission mode suitable to ISAC is still one of the future research trends.

B. ISAC Signal Processing

ISAC signal processing includes single-BS sensing algorithms and multi-BS cooperative sensing algorithms. High sensing accuracy and low computational complexity are the two most critical performance metrics pursued by ISAC signal processing algorithms. The ISAC signal processing algorithm will be the tradeoff between these two performance indices. For new applications, such as intelligent transportation and smart city, multi-BS cooperative sensing is the key technology to realize large-scale and high-accuracy sensing. The design of a cooperative sensing algorithm is challenging.

1) ISAC Signal Processing With High Accuracy and Low Complexity: There is a tradeoff between the complexity and accuracy when designing ISAC signal processing algorithms. Ma et al. [144] analyzed the sensing performance of the existing frame structure using different reference signals. However, since there are multiple reference signals, the effective application of these reference signals is still an open problem. In the future, the ISAC systems on the mmWave and THz bands will be common [145]. Hence, the high-accurate ISAC signal processing algorithms on mmWave and THz bands are the future research trends.

2) Cooperative Signal Processing: The networked mobile communication system is applied to realize cooperative sensing using multiple BSs, which can significantly improve the sensing accuracy and range [146]. Correspondingly, the signal processing for cooperative sensing needs to be studied. Most existing cooperative sensing methods are designed for pulse radar or coherent radar. Take the coherent radar as an example, the signals transmitted by each radar are adjusted to the same frequency and phase when they reach the target, which greatly improves the SNR of the echo signal [147]. Coherent radar requires high time and phase synchronization, whose signal processing methods are unsuitable for mobile communication systems with ISAC capability. There are few existing studies on cooperative sensing methods for ISAC systems. Hence, the signal processing for cooperative sensing and communication system is one of the future trends.

C. ISAC Signal Optimization

The ISAC signal design mainly focuses on the research of modulation and multiplexing methods, and there is no flexible and reconfigurable ISAC design combined with the frame structure. Besides, there are no comprehensive signal optimization schemes in the space–time–frequency domains. The goal of spatial optimization is to design the ISAC beams into ideal directions to improve the performance of sensing and communication. Optimization in the time–frequency domains focuses on the subcarrier and power allocation of ISAC signals. The ISAC signal optimization in the space–time–frequency domains simultaneously optimizes the precoding matrix, subcarrier allocation, power allocation, frame structure, etc., to obtain an ISAC signal with approximate ideal performance. In addition, there are limited studies on ISAC signal optimization for multi-BS cooperative sensing. Overall, under the differentiated requirements of communication and sensing in diversified scenarios, the ISAC signal optimization in space–time–frequency multi-domain is the future trend. Besides, to extend the sensing range and improve the sensing accuracy, further in-depth research on ISAC signal optimization for cooperative sensing is required.

VI. Conclusion

ISAC has been regarded as one of the potential key technologies of future mobile communication systems, with ISAC signal as the fundamental technology. In this article, we review ISAC signals in the perspective of 5G, 5G-A, and 6G mobile communication systems from three aspects, namely, signal design, signal processing, and signal optimization. In the future, facing the various scenarios in the era of 5G-A and 6G, flexible and reconfigurable ISAC signals need to be designed. This article comprehensively reviews the ISAC signals, which may provide a guideline for researchers in the area of ISAC technology.

References

[1] Z. Feng, Z. Fang, Z. Wei, X. Chen, Z. Quan, and D. Ji, "Joint radar and communication: A survey," *China Commun.*, vol. 17, no. 1, pp. 1–27, Jan. 2020.

[2] M. M. Şahin and H. Arslan, "Multi-functional coexistence of radar-sensing and communication waveforms," in *Proc. IEEE 92nd Veh. Technol. Conf. (VTC-Fall)*, 2020, pp. 1–5.

[3] H. T. Hayvaci and B. Tavli, "Spectrum sharing in radar and wireless communication systems: A review," in *Proc. Int. Conf. Electromagn. Adv. Appl. (ICEAA)*, 2014, pp. 810–813.

[4] A. R. Chiriyath, B. Paul, and D. W. Bliss, "Radar-communications convergence: Coexistence, cooperation, and co-design," *IEEE Trans. Cogn. Commun. Netw.*, vol. 3, no. 1, pp. 1–12, Mar. 2017.

[5] F. Liu, C. Masouros, A. P. Petropulu, H. Griffiths, and L. Hanzo, "Joint radar and communication design: Applications, state-of-the-art, and the road ahead," *IEEE Trans. Commun.*, vol. 68, no. 6, pp. 3834–3862, Jun. 2020.

[6] J. A. Zhang et al., "An overview of signal processing techniques for joint communication and radar sensing," 2021, *arXiv:2102.12780*.

[7] H. Griffiths et al., "Radar spectrum engineering and management: Technical and regulatory issues," *Proc. IEEE*, vol. 103, no. 1, pp. 85–102, Jan. 2015.

[8] S. Quan, W. Qian, J. Guq, and V. Zhang, "Radar-communication integration: An overview," in *Proc. 7th IEEE Int. Conf. Adv. Infocomm Technol.*, 2014, pp. 98–103.

[9] R. M. Mealey, "A method for calculating error probabilities in a radar communication system," *IEEE Trans. Space Electron. Telemetry*, vol. SET-9, no. 2, pp. 37–42, Jun. 1963.

[10] M. Scharrenbroich and M. Zatman, "Joint radar-communications resource management," in *Proc. IEEE Radar Conf. (RadarConf)*, 2016, pp. 1–6.

[11] C. B. Barneto et al., "Full-duplex OFDM radar with LTE and 5G NR waveforms: Challenges, solutions, and measurements," *IEEE Trans. Microw. Theory Techn.*, vol. 67, no. 10, pp. 4042–4054, Oct. 2019.

[12] "Introduction to 6G | IMT-2030." Apr. 2020. [Online]. Available: https://www.tonex.com/training-courses/introduction-to-6g-imt-2030/

[13] S. Xu, B. Chen, and P. Zhang, "Radar-communication integration based on DSSS techniques," in *Proc. 8th Int. Conf. Signal Process.*, vol. 4, 2006.

[14] C. Sturm, T. Zwick, and W. Wiesbeck, "An OFDM system concept for joint radar and communications operations," in *Proc. VTC Spring IEEE 69th Veh. Technol. Conf.*, 2009, pp. 1–5.

[15] C. Sturm, T. Zwick, W. Wiesbeck, and M. Braun, "Performance verification of symbol-based OFDM radar processing," in *Proc. IEEE Radar Conf.*, 2010, pp. 60–63.

[16] Y. L. Sit, L. Reichardt, C. Sturm, and T. Zwick, "Extension of the OFDM joint radar-communication system for a multipath, multiuser scenario," in *Proc. IEEE RadarCon (RADAR)*, 2011, pp. 718–723.

[17] Y. Zhou, H. Zhou, F. Zhou, Y. Wu, and V. C. M. Leung, "Resource allocation for a wireless powered integrated radar and communication system," *IEEE Wireless Commun. Lett.*, vol. 8, no. 1, pp. 253–256, Feb. 2019.

[18] S. Koslowski, M. Braun, and F. K. Jondral, "Using filter bank multicarrier signals for radar imaging," in *Proc. IEEE/ION Position Location Navig. Symp. (PLANS)*, 2014, pp. 152–157.

[19] R. Hadani et al., "Orthogonal time frequency space modulation," in *Proc. IEEE Wireless Commun. Netw. Conf. (WCNC)*, 2017, pp. 1–6.

[20] J. B. Sanson, D. Castanheira, A. Gameiro, and P. P. Monteiro, "Non-orthogonal multicarrier waveform for radar with communications systems: 24 GHz GFDM RadCom," *IEEE Access*, vol. 7, pp. 128694–128705, 2019.

[21] X. Yuan et al., "Spatio-temporal power optimization for MIMO joint communication and radio sensing systems with training overhead," *IEEE Trans. Veh. Technol.*, vol. 70, no. 1, pp. 514–528, Jan. 2021.

[22] X. Yuan, Z. Feng, W. Ni, Z. Wei, and R. P. Liu, "Waveform optimization for MIMO joint communication and radio sensing systems with imperfect channel feedbacks," in *Proc. IEEE Int. Conf. Commun. Workshops (ICC Workshops)*, 2020, pp. 1–6.

[23] J. A. Zhang et al., "Enabling joint communication and radar sensing in mobile networks—A survey," *IEEE Commun. Surveys Tuts.*, vol. 24, no. 1, pp. 306–345, 1st Quart., 2022.

[24] Z. Wang et al., "Symbiotic sensing and communications towards 6G: Vision, applications, and technology trends," in *Proc. IEEE 94th Veh. Technol. Conf. (VTC-Fall)*, 2021, pp. 1–5.

[25] D. K. P. Tan et al., "Integrated sensing and communication in 6G: Motivations, use cases, requirements, challenges and future directions," in *Proc. 1st IEEE Int. Online Symp. Joint Commun. Sens. (JC S)*, 2021, pp. 1–6.

[26] J. Xiong, H. Yin, J. Zhu, and Y. Tang, "An overview of waveform design for integrated sensing and communication," in *Proc. IEEE/CIC Int. Conf. Commun. China (ICCC)*, 2022, pp. 991–996.

[27] L. Hu, Z. Du, and G. Xue, "Radar-communication integration based on OFDM signal," in *Proc. IEEE Int. Conf. Signal Process. Commun. Comput. (ICSPCC)*, 2014, pp. 442–445.

[28] W. Cao, J. Zhu, X. Li, W. Hu, and J. Lei, "Feasibility of multi-carrier modulation signals as new illuminators of opportunity for passive radar: Orthogonal frequency division multiplexing versus filter-bank multicarrier," *IET Radar Sonar Navig.*, vol. 10, no. 6, pp. 1080–1087, 2016.

[29] R. Gerzaguet et al., "The 5G candidate waveform race: A comparison of complexity and performance," *EURASIP J. Wireless Commun. Netw.*, vol. 2017, no. 1, pp. 1–14, 2017.

[30] P. Raviteja, K. T. Phan, Y. Hong, and E. Viterbo, "Interference cancellation and iterative detection for orthogonal time frequency space modulation," *IEEE Trans. Wireless Commun.*, vol. 17, no. 10, pp. 6501–6515, Oct. 2018.

[31] L. Gaudio, M. Kobayashi, G. Caire, and G. Colavolpe, "On the effectiveness of OTFS for joint radar parameter estimation and communication," *IEEE Trans. Wireless Commun.*, vol. 19, no. 9, pp. 5951–5965, Sep. 2020.

[32] D. R. Wehner, *High Resolution Radar*. Norwood, MA, USA: Artech House, 1987.

[33] S. Stein, "Algorithms for ambiguity function processing," *IEEE Trans. Acoust., Speech, Signal Process.*, vol. ASSP-29, no. 3, pp. 588–599, Jun. 1981.

[34] Y. Zhao and S.-G. Haggman, "Sensitivity to Doppler shift and carrier frequency errors in OFDM systems-the consequences and solutions," in *Proc. Veh. Technol. Conf. (VTC)*, vol. 3, 1996, pp. 1564–1568.

[35] J. A. Johnston and A. C. Fairhead, "Waveform design and Doppler sensitivity analysis for nonlinear FM chirp pulses," in *IEE Proc. F, Commun. Radar Signal Process.*, vol. 133, no. 2, pp. 163–175, 1986.

[36] G. E. A. Franken, H. Nikookar, and P. Van Genderen, "Doppler tolerance of OFDM-coded radar signals," in *Proc. Eur. Radar Conf.*, 2006, pp. 108–111.

[37] S. H. Han and J. H. Lee, "PAPR reduction of OFDM signals using a reduced complexity PTS technique," *IEEE Signal Process. Lett.*, vol. 11, no. 11, pp. 887–890, Nov. 2004.

[38] Y. Liu, G. Liao, J. Xu, Z. Yang, and Y. Zhang, "Adaptive OFDM integrated radar and communications waveform design based on information theory," *IEEE Commun. Lett.*, vol. 21, no. 10, pp. 2174–2177, Oct. 2017.

[39] M. Li, W.-Q. Wang, and Z. Zheng, "Communication-embedded OFDM chirp waveform for delay-Doppler radar," *IET Radar Sonar Navig.*, vol. 12, no. 3, pp. 353–360, 2018.

[40] M. B. Alabd, B. Nuss, C. Winkler, and T. Zwick, "Partial chirp modulation technique for chirp sequence based radar communications," in *Proc. 16th Eur. Radar Conf. (EuRAD)*, 2019, pp. 173–176.

[41] Z. Zhang, Y. Qu, Z. Wu, M. J. Nowak, J. Ellinger, and M. C. Wicks, "RF steganography via LFM chirp radar signals," *IEEE Trans. Aerosp. Electron. Syst.*, vol. 54, no. 3, pp. 1221–1236, Jun. 2018.

[42] P. Striano, C. V. Ilioudis, C. Clemente, and J. J. Soraghan, "Performance of a communicating radar using FSK and fractional Fourier transform for automotive applications," in *Proc. IEEE Radio Wireless Symp. (RWS)*, 2019, pp. 1–4.

[43] X. Tian, T. Zhang, Q. Zhang, and Z. Song, "Waveform design and processing in OFDM based radar-communication integrated systems," in *Proc. IEEE/CIC Int. Conf. Commun. China (ICCC)*, 2017, pp. 1–6.

[44] J. Zhao, K. Huo, and X. Li, "A chaos-based phase-coded OFDM signal for joint radar-communication systems," in *Proc. 12th Int. Conf. Signal Process. (ICSP)*, 2014, pp. 1997–2002.

[45] S. H. Dokhanchi, M. R. B. Shankar, T. Stifter, and B. Ottersten, "Multicarrier phase modulated continuous waveform for automotive joint radar-communication system," in *Proc. IEEE 19th Int. Workshop Signal Process. Adv. Wireless Commun. (SPAWC)*, 2018, pp. 1–5.

[46] F. Uysal, "Phase-coded FMCW automotive radar: System design and interference mitigation," *IEEE Trans. Veh. Technol.*, vol. 69, no. 1, pp. 270–281, Jan. 2020.

[47] S. Y. Nusenu, W.-Q. Wang, and A. Basit, "Time-modulated FD-MIMO array for integrated radar and communication systems," *IEEE Antennas Wireless Propag. Lett.*, vol. 17, pp. 1015–1019, 2018.

[48] J.-H. Kim, M. Younis, A. Moreira, and W. Wiesbeck, "A novel OFDM chirp waveform scheme for use of multiple transmitters in SAR," *IEEE Geosci. Remote Sens. Lett.*, vol. 10, no. 3, pp. 568–572, May 2013.

[49] S.-J. Cheng, W.-Q. Wang, and H.-Z. Shao, "Spread spectrum-coded OFDM chirp waveform diversity design," *IEEE Sensors J.*, vol. 15, no. 10, pp. 5694–5700, Oct. 2015.

[50] S. Sharma, M. Melvasalo, and V. Koivunen, "Multicarrier DS-CDMA waveforms for joint radar-communication system," in *Proc. IEEE Radar Conf. (RadarConf)*, 2020, pp. 1–6.

[51] D. Sidney, "Pulse transmission," U.S. Patent 2 678 997, May 18, 1954.

[52] C. E. Cook, "Linear FM signal formats for beacon and communication systems," *IEEE Trans. Aerosp. Electron. Syst.*, vol. AES-10, no. 4, pp. 471–478, Jul. 1974.

[53] T. Takahashi, Y. Kato, K. Isoda, Y. Kitsukawa, and M. Mitsumoto, "A novel waveform for joint radar and communication systems," in *Proc. Int. Symp. Antennas Propag. (ISAP)*, 2019, pp. 1–3.

[54] D. Dash, A. Jayaprakash, J. Valarmathi, and G. R. Reddy, "Generalized OFDM-LFM waveform design and analysis for multistatic airborne radar," in *Proc. IEEE Power Commun. Inf. Technol. Conf. (PCITC)*, 2015, pp. 924–929.

[55] W.-Q. Wang, "An orthogonal frequency division multiplexing radar waveform with a large time-bandwidth product," *Defence Sci. J.*, vol. 62, no. 6, pp. 427–430, 2012.

[56] M. Winkler, *Chirp Signals for Communication*, WESCON, Wichita, KS, USA, 1962.

[57] C.-H. Wang and O. Altintas, "Demo: A joint radar and communication system based on commercially available FMCW radar," in *Proc. IEEE Veh. Netw. Conf. (VNC)*, 2018, pp. 1–2.

[58] S. Dwivedi, A. N. Barreto, P. Sen, and G. Fettweis, "Target detection in joint frequency modulated continuous wave (FMCW) radar-communication system," in *Proc. 16th Int. Symp. Wireless Commun. Syst. (ISWCS)*, 2019, pp. 277–282.

[59] X. Lv, J. Wang, Z. Jiang, and W. Wu, "A joint radar-communication system based on OCDM-OFDM scheme," in *Proc. Int. Conf. Microw. Millimeter Wave Technol. (ICMMT)*, 2018, pp. 1–3.

[60] K. Chen, Y. Liu, and W. Zhang, "Study on integrated radar-communication signal of OFDM-LFM based on FRFT," in *Proc. IET Int. Radar Conf.*, 2015, pp. 1–6.

[61] L. Qi, Y. Yao, B. Huang, and G. Wu, "A phase-coded OFDM signal for radar-communication integration," in *Proc. IEEE Int. Symp. Phased Array Syst. Technol. (PAST)*, 2019, pp. 1–4.

[62] Y. Zhang, Q. Li, L. Huang, and J. Song, "Waveform design for joint radar-communication system with multi-user based on MIMO radar," in *Proc. IEEE Radar Conf. (RadarConf)*, 2017, pp. 415–418.

[63] C. Sahin, J. Jakabosky, P. M. McCormick, J. G. Metcalf, and S. D. Blunt, "A novel approach for embedding communication symbols into physical radar waveforms," in *Proc. IEEE Radar Conf. (RadarConf)*, 2017, pp. 1498–1503.

[64] S. H. Dokhanchi, B. S. Mysore, K. V. Mishra, and B. Ottersten, "A mmwave automotive joint radar-communications system," *IEEE Trans. Aerosp. Electron. Syst.*, vol. 55, no. 3, pp. 1241–1260, 2019.

[65] S.-J. Cheng, W.-Q. Wang, and H. Shao, "MIMO OFDM chirp waveform design with spread spectrum modulation," in *Proc. IEEE China Summit Int. Conf. Signal Inf. Process. (ChinaSIP)*, 2014, pp. 208–211.

[66] H. Ma, X. Sun, and W. Jin, "Integrated waveform design based on spread spectrum OFDM radar communication," in *Proc. IEEE 3rd Adv. Inf. Manag. Commun. Electron. Autom. Control Conf. (IMCEC)*, 2019, pp. 1258–1263.

[67] T. Liang, Z. Li, M. Wang, and X. Fang, "Design of radar-communication integrated signal based on OFDM," in *Proc. Int. Conf. Artif. Intell. Commun. Netw.*, 2019, pp. 108–119.

[68] L. Tang, K. Zhang, H. Dai, P. Zhu, and Y.-C. Liang, "Analysis and optimization of ambiguity function in radar-communication integrated systems using MPSK-DSSS," *IEEE Wireless Commun. Lett.*, vol. 8, no. 6, pp. 1546–1549, Dec. 2019.

[69] X. Tian and Z. Song, "On radar and communication integrated system using OFDM signal," in *Proc. IEEE Radar Conf. (RadarConf)*, 2017, pp. 318–323.

[70] S. H. Dokhanchi, M. R. B. Shankar, K. V. Mishra, T. Stifter, and B. Ottersten, "Performance analysis of mmWave bi-static PMCW-based automotive joint radar-communications system," in *Proc. IEEE Radar Conf. (RadarConf)*, 2019, pp. 1–6.

[71] S. H. Dokhanchi, B. S. Mysore, K. V. Mishra, and B. Ottersten, "A mmWave automotive joint radar-communications system," *IEEE Trans. Aerosp. Electron. Syst.*, vol. 55, no. 3, pp. 1241–1260, Jun. 2019.

[72] X. Shen, R. Yang, X. Li, and M. Huang, "The research on DS-OFDM in integrated radar and communication," in *Wireless Communications, Networking and Applications*. New Delhi, India: Springer, 2016, pp. 729–740.

[73] N. Michailow, I. Gaspar, S. Krone, M. Lentmaier, and G. Fettweis, "Generalized frequency division multiplexing: Analysis of an alternative multi-carrier technique for next generation cellular systems," in *Proc. Int. Symp. Wireless Commun. Syst. (ISWCS)*, 2012, pp. 171–175.

[74] Y. Ha, W. Niu, and N. Chi, "Post equalization scheme based on deep neural network for a probabilistic shaping 128 QAM DFT-S OFDM signal in underwater visible light communication system," in *Proc. 18th Int. Conf. Opt. Commun. Netw. (ICOCN)*, 2019, pp. 1–3.

[75] D. Lee, A. Davydov, B. Mondal, G. Xiong, G. Morozov, and J. Kim, "From sub-terahertz to terahertz: Challenges and design considerations," in *Proc. IEEE Wireless Commun. Netw. Conf. Workshops (WCNCW)*, 2020, pp. 1–8.

[76] K. M. S. Huq, S. A. Busari, J. Rodriguez, V. Frascolla, W. Bazzi, and D. C. Sicker, "Terahertz-enabled wireless system for beyond-5G ultra-fast networks: A brief survey," *IEEE Netw.*, vol. 33, no. 4, pp. 89–95, Jul./Aug. 2019.

[77] G. Berardinelli, "Generalized DFT-s-OFDM waveforms without cyclic prefix," *IEEE Access*, vol. 6, pp. 4677–4689, 2017.

[78] M. Shi, F. Wang, M. Zhang, Z. Wang, and N. Chi, "PAPR reduction of 2.0Gbit/s DFT-S OFDM modulated visible light communication system based on interleaved sub-banding technique," in *Proc. IEEE Int. Conf. Commun. Workshops (ICC Workshops)*, 2017, pp. 337–342.

[79] L. Gaudio, M. Kobayashi, B. Bissinger, and G. Caire, "Performance analysis of joint radar and communication using OFDM and OTFS," in *Proc. IEEE Int. Conf. Commun. Workshops (ICC Workshops)*, 2019, pp. 1–6.

[80] P. Raviteja, K. T. Phan, Y. Hong, and E. Viterbo, "Orthogonal time frequency space (OTFS) modulation based radar system," in *Proc. IEEE Radar Conf. (RadarConf)*, 2019, pp. 1–6.

[81] W. Yuan, Z. Wei, S. Li, J. Yuan, and D. W. K. Ng, "Integrated sensing and communication-assisted orthogonal time frequency space transmission for vehicular networks," 2021, *arXiv:2105.03125*.

[82] U. Tureli, H. Liu, and M. D. Zoltowski, "OFDM blind carrier offset estimation: ESPRIT," *IEEE Trans. Commun.*, vol. 48, no. 9, pp. 1459–1461, Sep. 2000.

[83] K. Wu, J. A. Zhang, X. Huang, and Y. J. Guo, "Integrating low-complexity and flexible sensing into communication systems," 2021, *arXiv:2109.04109*.

[84] A. V. Oppenheim, *Applications of Digital Signal Processing*. Englewood Cliffs, NJ, USA: Prentice-Hall, 1978.

[85] R. Prony, "Essai experimental et analytique, etc," *J. de L'Ecole Polytechnique*, vol. 2, no. 1, pp. 24–76, 1795.

[86] R. Schmidt, "Multiple emitter location and signal parameter estimation," *IEEE Trans. Antennas Propag.*, vol. 34, no. 3, pp. 276–280, Mar. 1986.

[87] R. Roy, A. Paulraj, and T. Kailath, "ESPRIT—A subspace rotation approach to estimation of parameters of cisoids in noise," *IEEE Trans. Acoust., Speech, Signal Process.*, vol. ASSP-34, no. 5, pp. 1340–1342, Oct. 1986.

[88] J. Capon, "High-resolution frequency-wavenumber spectrum analysis," *Proc. IEEE*, vol. 57, no. 8, pp. 1408–1418, Aug. 1969.

[89] L. L. Scharf and L. T. McWhorter, "Geometry of the Cramer-Rao bound," *Signal Process.*, vol. 31, no. 3, pp. 301–311, 1993.

[90] C. Sturm and W. Wiesbeck, "Waveform design and signal processing aspects for fusion of wireless communications and radar sensing," *Proc. IEEE*, vol. 99, no. 7, pp. 1236–1259, Jul. 2011.

[91] Y. Zeng, Y. Ma, and S. Sun, "Joint radar-communication with cyclic prefixed single carrier waveforms," *IEEE Trans. Veh. Technol.*, vol. 69, no. 4, pp. 4069–4079, Apr. 2020.

[92] M. M. Ali and M. K. Alghrairi, "Minimizing of error detection using bartlett-DCT periodogram in cognitive radio networks," *J. Commun.*, vol. 14, no. 5, pp. 363–367, 2019.

[93] S. Dwivedi, A. Kota, and A. K. Jagannatham, "Optimal bartlett detector based SPRT for spectrum sensing in multi-antenna cognitive radio systems," *IEEE Signal Process. Lett.*, vol. 22, no. 9, pp. 1409–1413, Sep. 2015.

[94] J. Sanson, A. Gameiro, D. Castanheira, and P. P. Monteiro, "Comparison of DoA algorithms for MIMO OFDM radar," in *Proc. 15th Eur. Radar Conf. (EuRAD)*, 2018, pp. 226–229.

[95] M. Braun, C. Sturm, and F. K. Jondral, "Maximum likelihood speed and distance estimation for OFDM radar," in *Proc. IEEE Radar Conf.*, 2010, pp. 256–261.

[96] R. Couillet and M. Debbah, "A maximum entropy approach to OFDM channel estimation," in *Proc. IEEE 10th Workshop Signal Process. Adv. Wireless Commun.*, 2009, pp. 166–170.

[97] X. Chen, Z. Feng, Z. Wei, P. Zhang, and X. Yuan, "Code-division OFDM joint communication and sensing system for 6G machine-type communication," *IEEE Internet Things J.*, vol. 8, no. 15, pp. 12093–12105, Aug. 2021.

[98] L. Gaudio, M. Kobayashi, G. Caire, and G. Colavolpe, "Joint radar target detection and parameter estimation with MIMO OTFS," in *Proc. IEEE Radar Conf. (RadarConf)*, 2020, pp. 1–6.

[99] R. F. Tigrek, W. J. A. De Heij, and P. Van Genderen, "Relation between the peak to average power ratio and Doppler sidelobes of the multi-carrier radar signal," in *Proc. Int. Radar Conf. Surveillance Safer World (RADAR)*, 2009, pp. 1–6.

[100] W. Li, Z. Xiang, and P. Ren, "Waveform design for dual-function radar-communication system with Golay block coding," *IEEE Access*, vol. 7, pp. 184053–184062, 2019.

[101] R. F. Tigrek and P. Van Genderen, "A Golay code based approach to reduction of the PAPR and its consequence for the data throughput," in *Proc. Eur. Radar Conf.*, 2007, pp. 146–149.

[102] X. Tian, T. Zhang, Q. Zhang, and Z. Song, "HRRP-based extended target recognition in OFDM-based RadCom systems," in *Proc. IEEE Global Commun. Conf. (GLOBECOM)*, 2018, pp. 1–6.

[103] H. Zhao and W. Zou, "Judgement-based joint SLM and PTS algorithm for PAPR suppression of radar communication integrated system," in *Proc. IEEE/CIC Int. Conf. Commun. China (ICCC Workshops)*, 2018, pp. 131–135.

[104] S. Y. Le Goff, S. S. Al-Samahi, B. K. Khoo, C. C. Tsimenidis, and B. S. Sharif, "Selected mapping without side information for PAPR reduction in OFDM," *IEEE Trans. Wireless Commun.*, vol. 8, no. 7, pp. 3320–3325, Jul. 2009.

[105] X. Lv, J. Wang, Z. Jiang, and W. Jiao, "A novel PAPR reduction method for OCDM-based radar-communication signal," in *Proc. IEEE MTT-S Int. Microw. Workshop Series 5G Hardw. Syst. Technol. (IMWS-5G)*, 2018, pp. 1–3.

[106] K. V. Rema, N. Rajeev, and M. K. Manoj, "MIMO OCDM with reduced PAPR," in *Proc. Int. Conf. Intell. Comput. Control (I2C2)*, 2017, pp. 1–6.

[107] Y. L. Sit, C. Sturm, and T. Zwick, "Interference cancellation for dynamic range improvement in an OFDM joint radar and communication system," in *Proc. 8th Eur. Radar Conf.*, 2011, pp. 333–336.

[108] Y. L. Sit, C. Sturm, and T. Zwick, "One-stage selective interference cancellation for the OFDM joint radar-communication system," in *Proc. 7th German Microw. Conf.*, 2012, pp. 1–4.

[109] Y. L. Sit, B. Nuss, and T. Zwick, "On mutual interference cancellation in a MIMO OFDM multiuser radar-communication network," *IEEE Trans. Veh. Technol.*, vol. 67, no. 4, pp. 3339–3348, Apr. 2018.

[110] Y. Zeng, Y. Ma, and S. Sun, "Joint radar-communication: Low complexity algorithm and self-interference cancellation," in *Proc. IEEE Global Commun. Conf. (GLOBECOM)*, 2018, pp. 1–7.

[111] Y. Zhang, Q. Wang, H. Qin, and J. Meng, "Adaptive self-interference cancellation system for microwave LFMCW radar with optimal delay matching," in *Proc. Joint Int. Symp. Electromagn. Compat. Sapporo Asia–Pacific Int. Symp. Electromagn. Compat. (EMC Sapporo/APEMC)*, 2019, pp. 729–732.

[112] K. U. Mazher, T. Shimizu, R. W. Heath, and G. Bansal, "Automotive radar using IEEE 802.11p signals," in *Proc. IEEE Wireless Commun. Netw. Conf. (WCNC)*, 2018, pp. 1–6.

[113] C. B. Barneto et al., "High-accuracy radio sensing in 5G new radio networks: Prospects and self-interference challenge," in *Proc. 53rd Asilomar Conf. Signals Syst. Comput.*, 2019, pp. 1159–1163.

[114] H. Hellsten and E. Nilsson, "Multiple access radar using slow chirp modulation," in *Proc. IEEE Radar Conf. (RadarConf)*, 2020, pp. 1–6.

[115] M. Lübke, J. Fuchs, V. Shatov, A. Dubey, R. Weigel, and F. Lurz, "Combining radar and communication at 77 GHz using a CDMA technique," in *Proc. IEEE MTT-S Int. Conf. Microw. Intell. Mobility (ICMIM)*, 2020, pp. 1–4.

[116] S. Hadizadehmoghaddam and R. S. Adve, "Simultaneous execution of multiple radar tasks using OFDMA," in *Proc. IEEE Radar Conf. (RadarConf)*, 2017, pp. 622–626.

[117] S. Hadizadehmoghaddam, F. Yusufali, and R. S. Adve, "Interference-aware power allocation in OFDMA radar," in *Proc. IEEE Radar Conf. (RadarConf)*, 2018, pp. 821–826.

[118] M. Kurosawa, T. Nozawa, M. Umehira, X. Wang, S. Takeda, and H. Kuroda, "Proposal of multiple access FMCW radar for inter-radar interference avoidance," *J. Eng.*, vol. 2019, no. 21, pp. 7304–7308, 2019.

[119] S. Ishikawa, M. Kurosawa, M. Umehira, W. Xiaoyan, S. Takeda, and H. Kuroda, "Packet-based FMCW radar using CSMA technique to avoid narrowband interefrence," in *Proc. Int. Radar Conf. (RADAR)*, 2019, pp. 1–5.

[120] M. Goppelt, H.-L. Blöcher, and W. Menzel, "Automotive radar–investigation of mutual interference mechanisms," *Adv. Radio Sci.*, vol. 8, no. B3, pp. 55–60, 2010.

[121] A. Tang, S. Li, and X. Wang, "Self-interference-resistant IEEE 802.11ad-based joint communication and automotive radar design," *IEEE J. Sel. Topics Signal Process.*, vol. 15, no. 6, pp. 1484–1499, Nov. 2021.

[122] F. Lehmann, "A message-passing receiver for OFDM-based self-interference-limited networks," *IEEE Trans. Veh. Technol.*, vol. 65, no. 8, pp. 6136–6145, Aug. 2016.

[123] D. P. Zilz and M. R. Bell, "Statistical modeling of wireless communications interference and its effects on adaptive-threshold radar detection," *IEEE Trans. Aerosp. Electron. Syst.*, vol. 54, no. 2, pp. 890–911, Apr. 2018.

[124] F. Liu, C. Masouros, A. Li, H. Sun, and L. Hanzo, "MU-MIMO communications with MIMO radar: From co-existence to joint transmission," *IEEE Trans. Wireless Commun.*, vol. 17, no. 4, pp. 2755–2770, Apr. 2018.

[125] F. Liu, L. Zhou, C. Masouros, A. Li, W. Luo, and A. Petropulu, "Toward dual-functional radar-communication systems: Optimal waveform design," *IEEE Trans. Signal Process.*, vol. 66, no. 16, pp. 4264–4279, Aug. 2018.

[126] H. Hua, J. Xu, and T. X. Han, "Optimal transmit beamforming for integrated sensing and communication," 2021, *arXiv:2104.11871*.

[127] Z. Zhang, Z. Du, and W. Yu, "Mutual-information-based OFDM waveform design for integrated radar-communication system in Gaussian mixture clutter," *IEEE Sensors Lett.*, vol. 4, no. 1, pp. 1–4, Jan. 2020.

[128] Y. Chen, Y. Nijsure, C. Yuen, Y. H. Chew, Z. Ding, and S. Boussakta, "Adaptive distributed MIMO radar waveform optimization based on mutual information," *IEEE Trans. Aerosp. Electron. Syst.*, vol. 49, no. 2, pp. 1374–1385, Apr. 2013.

[129] M. F. Keskin et al., "Peak sidelobe level based waveform optimization for OFDM joint radar-communications," in *Proc. 17th Eur. Radar Conf. (EuRAD)*, 2021, pp. 1–4.

[130] S. Zhu, X. Li, R. Yang, and Y. Ding, "Adaptive waveform optimization method for OFDM radar communication jamming," in *Proc. IEEE Int. Conf. Consum. Electron. Comput. Eng. (ICCECE)*, 2021, pp. 600–605.

[131] Y. Liu, G. Liao, Z. Yang, and J. Xu, "Multiobjective optimal waveform design for OFDM integrated radar and communication systems," *Signal Process.*, vol. 141, pp. 331–342, Dec. 2017.

[132] M. Mousaei, M. Soltanalian, and B. Smida, "ComSens: Exploiting pilot diversity for pervasive integration of communication and sensing in MIMO-TDD-frameworks," in *Proc. IEEE Mil. Commun. Conf. (MILCOM)*, 2017, pp. 617–622.

[133] Z. Wei et al., "5G PRS-based sensing: A sensing reference signal approach for joint sensing and communication system," *IEEE Trans. Veh. Technol.*, early access, Oct. 17, 2022, doi: 10.1109/TVT.2022.3215159.

[134] P. Kumari, J. Choi, N. González-Prelcic, and R. W. Heath, "IEEE 802.11ad-based radar: An approach to joint vehicular communication-radar system," *IEEE Trans. Veh. Technol.*, vol. 67, no. 4, pp. 3012–3027, Apr. 2018.

[135] G. Liu et al., "Integration of communication and SAR radar based on OFDM with channel estimation in high speed scenario," in *Proc. IEEE Int. Geosci. Remote Sens. Symp. (IGRSS)*, 2019, pp. 2519–2522.

[136] C. D. Ozkaptan, E. Ekici, O. Altintas, and C.-H. Wang, "OFDM pilot-based radar for joint vehicular communication and radar systems," in *Proc. IEEE Veh. Netw. Conf. (VNC)*, 2018, pp. 1–8.

[137] D. Bao, G. Qin, and Y.-Y. Dong, "A superimposed pilot-based integrated radar and communication system," *IEEE Access*, vol. 8, pp. 11520–11533, 2020.

[138] C.-H. Wang, O. Altintas, C. D. Ozkaptan, and E. Ekici, "Multi-range joint automotive radar and communication using pilot-based OFDM radar," in *Proc. IEEE Veh. Netw. Conf. (VNC)*, 2020, pp. 1–4.

[139] H. Soury and B. Smida, "Optimal pilot overhead for FDD full-duplex communication and radar sensing (ComSens)," in *Proc. IEEE Mil. Commun. Conf. (MILCOM)*, 2017, pp. 725–730.

[140] R. Zhang, B. Shim, W. Yuan, M. Di Renzo, X. Dang, and W. Wu, "Integrated sensing and communication waveform design with sparse vector coding: Low sidelobes and ultra reliability," *IEEE Trans. Veh. Technol.*, vol. 71, no. 4, pp. 4489–4494, Apr. 2022.

[141] X. Wang, Z. Fei, J. Huang, and H. Yu, "Joint waveform and discrete phase shift design for RIS-assisted integrated sensing and communication system under cramér-Rao bound constraint," *IEEE Trans. Veh. Technol.*, vol. 71, no. 1, pp. 1004–1009, Jan. 2022.

[142] M. Babenko et al., "Efficient implementation of cryptography on points of an elliptic curve in residue number system," in *Proc. Int. Conf. Eng. Telecommun. (EnT)*, 2019, pp. 1–5.

[143] Z. Xiao and Y. Zeng, "Waveform design and performance analysis for full-duplex integrated sensing and communication," *IEEE J. Sel. Areas Commun.*, vol. 40, no. 6, pp. 1823–1837, Jun. 2022.
[144] L. Ma, C. Pan, Q. Wang, M. Lou, Y. Wang, and T. Jiang, "A downlink pilot based signal processing method for integrated sensing and communication towards 6G," in *Proc. IEEE 95th Veh. Technol. Conf. (VTC-Spring)*, 2022, pp. 1–5.
[145] O. Li et al., "Integrated sensing and communication in 6G a prototype of high resolution THz sensing on portable device," in *Proc. Joint Eur. Conf. Netw. Commun. 6G Summit (EuCNC/6G Summit)*, 2021, pp. 544–549.
[146] W. Jiang, Z. Wei, B. Li, Z. Feng, and Z. Fang, "Improve radar sensing performance of multiple roadside units cooperation via space registration," *IEEE Trans. Veh. Technol.*, vol. 71, no. 10, pp. 10975–10990, Oct. 2022.
[147] P. Yin, X. Yang, Q. Liu, and T. Long, "Wideband distributed coherent aperture radar," in *Proc. IEEE Radar Conf.*, 2014, pp. 1114–1117.

Zhiqing Wei (Member, IEEE) received the B.E. and Ph.D. degrees from Beijing University of Posts and Telecommunications (BUPT), Beijing, China, in 2010 and 2015, respectively.

He is an Associate Professor with BUPT. He has authored one book, three book chapters, and more than 50 papers. His research interest is the performance analysis and optimization of intelligent machine networks.

Dr. Wei was granted the Exemplary Reviewer of IEEE WIRELESS COMMUNICATIONS LETTERS in 2017 and the Best Paper Award of WCSP 2018. He was the Registration Co-Chair of IEEE/CIC ICCC 2018 and the Publication Co-Chair of IEEE/CIC ICCC 2019 and IEEE/CIC ICCC 2020.

Hanyang Qu (Member, IEEE) received the B.S. degree from the School of Electronic Engineering and Optoelectronic Technology, Nanjing University of Science and Technology, Nanjing, China, in 2020. He is currently pursuing the master's degree with Beijing University of Posts and Telecommunication, Beijing, China.

His research interests include integrated sensing and communication and high-accuracy sensing.

Yuan Wang (Member, IEEE) received the B.E. degree from the University of Science and Technology Beijing, Beijing, China, in 2020. She is currently pursuing the M.E. degree with the School of Information and Communication Engineering, Beijing University of Posts and Telecommunications, Beijing.

Her research interests include integrated sensing and communication.

Xin Yuan (Member, IEEE) received the B.E. degree from Taiyuan University of Technology, Taiyuan, Shanxi, China, in 2013, and the dual Ph.D. degree from Beijing University of Posts and Telecommunications, Beijing, China, and the University of Technology Sydney, Sydney, NSW, Australia, in 2019 and 2020, respectively.

She is currently a Research Scientist with CSIRO, Sydney. Her research interests include machine learning and optimization, and their applications to UAV networks and intelligent systems.

Huici Wu (Member, IEEE) received the Ph.D. degree from Beijing University of Posts and Telecommunications (BUPT), Beijing, China, in 2018.

From 2016 to 2017, she visited the Broadband Communications Research Group, University of Waterloo, Waterloo, ON, Canada. She is currently an Associate Professor with BUPT. Her research interests are in the area of wireless communications and networks, with current emphasis on collaborative air-to-ground communication and wireless access security.

Ying Du (Member, IEEE) is currently pursuing the Ph.D. degree with the University of Science and Technology of China, Hefei, China.

She is the Professor-Level Senior Engineer with the China Academy of Information and Communications Technology, Beijing, China. She is the Vice Chair of Standards and International Cooperation Working Group of IMT-2030(6G) Promotion Group. She has contributed to the research, evaluation, and international standardization of IEEE 802.16, 4G, 5G, and 6G communication systems. She has authored or coauthored more than 30 research papers or articles, and over 40 patents in this area. She has hosted three national major projects on mobile broadband system. She currently focuses on technology research, standardization, and verification for 5G-advanced and 6G systems.

Kaifeng Han (Member, IEEE) received the B.Eng. degree (First-Class Hons.) in electrical engineering from Beijing University of Posts and Telecommunications, Beijing, China, and Queen Mary University of London, London, U.K., in 2015, and the Ph.D. degree in electrical engineering from The University of Hong Kong, Hong Kong, in 2019.

He is a Senior Engineer with the China Academy of Information and Communications Technology, Beijing. He is funded by the China Association for Science and Technology Young Talent Support Program. He published over 40 research papers in international conferences and journals. His research interests focus on integrated sensing and communications, and wireless AI for 6G.

Dr. Han received one best paper award.

Ning Zhang (Senior Member, IEEE) received the Ph.D. degree in electrical and computer engineering from the University of Waterloo, Waterloo, ON, Canada, in 2015.

After that, he was a Postdoctoral Research Fellow with the University of Waterloo and the University of Toronto, Toronto, ON, Canada, respectively. Since 2020, he has been an Associate Professor with the Department of Electrical and Computer Engineering, University of Windsor, Windsor, ON, Canada. His research interests include connected vehicles, mobile-edge computing, wireless networking, and security.

Dr. Zhang received eight best paper awards from conferences and journals, such as IEEE Globecom, IEEE ICC, IEEE ICCC, IEEE WCSP, and *Journal of Communications and Information Networks*. He also received the IEEE TCSVC Rising Star Award and the IEEE ComSoc Young Professionals Outstanding Nominee Award. He is a Highly Cited Researcher (Web of Science). He serves/served as an Associate Editor for IEEE TRANSACTIONS ON MOBILE COMPUTING, IEEE INTERNET OF THINGS JOURNAL, IEEE TRANSACTIONS ON COGNITIVE COMMUNICATIONS AND NETWORKING, and IEEE SYSTEMS JOURNAL. He also serves/served as a TPC Chair for IEEE VTC 2021 and IEEE SAGC 2020, a General Chair for IEEE SAGC 2021, and a Chair for track of several international conferences and workshops, including IEEE ICC, VTC, INFOCOM Workshop, and Mobicom Workshop.

Zhiyong Feng (Senior Member, IEEE) received the B.E., M.E., and Ph.D. degrees from Beijing University of Posts and Telecommunications (BUPT), Beijing, China, in 1993, 1997, and 2009, respectively.

She is a Professor with BUPT, where she is also the Director of the Key Laboratory of the Universal Wireless Communications, Ministry of Education. Her main research interests include wireless network architecture design and radio resource management in 5th generation mobile networks (5G), spectrum sensing and dynamic spectrum management in cognitive wireless networks, and universal signal detection and identification.

Prof. Feng is the Vice Chair of the Information and Communication Test Committee of the Chinese Institute of Communications. She is currently serving as an Associate Editor-in-Chief for *China Communications*, and she is a Technological Advisor for international forum on NGMN.